

VIBRATIONS OF A CHAIN OF COUPLED  
BIFILAR PENDULUMS

A THESIS

Presented to

The Faculty of the Division of Graduate  
Studies and Research

by

Patricio Alban Maldonado

In Partial Fulfillment  
of the Requirements for the Degree  
Master of Science in Mechanical Engineering

Georgia Institute of Technology

November, 1974

VIBRATIONS OF A CHAIN OF COUPLED  
BIFILAR PENDULUMS

Approved:

*all*  
\_\_\_\_\_  
Allan D. Pierce, Chairman

*H. J. Johnson*  
\_\_\_\_\_  
Harold J. Johnson

*David McGill*  
\_\_\_\_\_  
David McGill

Date approved by Chairman: Nov. 11, 1974

## ACKNOWLEDGMENTS

I wish to express my sincere appreciation to my advisor, Dr. Allan D. Pierce, for his guidance and continued interest in this research. The consistent helpfulness of the other members of the thesis committee, Dr. Harold L. Johnson and Dr. David J. McGill, is gratefully acknowledged.

I also wish to thank my wife, Jenny, for her support throughout this work, and my parents, who supported me along eighteen years of study.

Finally, I am grateful to the Institute of International Education, and the State Department of the USA, for its financial support without which this research would not have been possible.

## TABLE OF CONTENTS

	Page
ACKNOWLEDGMENTS .....	ii
LIST OF TABLES .....	iv
LIST OF ILLUSTRATIONS .....	v
NOMENCLATURE .....	vii
SUMMARY .....	ix
Chapter	
I. INTRODUCTION .....	1
II. MATHEMATICAL MODEL .....	3
Force Analysis .....	3
Equation of Motion .....	13
Application of the Equations of Motion to the Real Model .....	18
III. EXPERIMENTAL MODEL .....	23
Calculations and Results .....	23
Design and Construction .....	29
IV. DATA AND COMPARISON WITH THEORY .....	55
Experimental Results .....	58
V. DISCUSSION AND CONCLUSIONS .....	64
APPENDIX I.....	67
BIBLIOGRAPHY .....	69

## LIST OF TABLES

Table		Page
1.	Values of $\Psi$ , $I_{zz}$ , and Corresponding Rod Shape .....	25
2.	Coefficients for Matrices $[P]$ .....	30
3.	Results for the Case $\Psi = 1.0$ .....	31
4.	Results for the Case $\Psi = 0.50$ .....	32
5.	Results for the Case $\Psi = -0.50$ .....	33
6.	Results for the Case $\Psi = -1.0$ .....	34
7.	Beam Frequencies .....	56

## LIST OF ILLUSTRATIONS

Figure	Page
1. Schematic View of the System .....	3
2. Force Distribution in the upper Elastic Members due only to Gravity. ....	5
3. Force Distribution Including Gravitational and Tension Forces .....	5
4. Final Force Distribution .....	6
5. Selected Model for Derivation .....	7
6. External Forces Acting on a Single Rod .....	7
7. Internal Forces .....	8
8. Restoring Forces .....	10
9. Inertial Translational Reaction Forces .....	11
10. Inertial Rotational Reaction Forces .....	11
11. Forces in the Horizontal Direction Acting on a Single Rod .....	13
12. Interactions of the Chain .....	19
13. Chain Motion for $\Psi = 1.0$ .....	35
14. Chain Motion for $\Psi = 0.5$ .....	36
15. Chain Motion for $\Psi = -0.5$ .....	37
16. Chain Motion for $\Psi = -1.0$ .....	38
17. Geometry of the Rod .....	39
18. a) Pinned Joints on the Chain .....	41
b) Sectional View of the Joints .....	41
c) Top View A-A .....	41
19. Eye-Screws at a Joint .....	42
20. a) Intermediate Rods .....	42
b) First and Last Rods .....	42

Figure	Page
21. Elastic Members .....	43
22. Cantilever Beam with Mass at End .....	46
23. Deflection of a Cantilever Beam .....	46
24. Force Analysis of a Cantilever Beam .....	47
25. Moment of Inertia of the Beam Section .....	48
26. Driving Mechanism	
a) Middle Section Front View .....	50
b) Side View .....	50
27. Beam-Rod Coupling	
a) Front View .....	51
b) Top View .....	51
28. Frame of the Model .....	52
29. Experimental Model.....	53
30. Driving Mechanism .....	54
31. Coupling of Beam to Chain .....	54
32. Beam Frequency Vs. Beam Length .....	57
33. Response Motion for $f = 1.5$ Hz.....	60
34. Response Motion for $f = 1.85$ Hz .....	60
35. Response Motion for $f = 2.4$ Hz .....	61
36. Response Motion for $f = 2.75$ Hz .....	61
37. Response Motion for $f = 3.1$ Hz .....	62
38. Response Motion for $f = 3.5$ Hz .....	62
39. Response Motion for $f = 4.0$ Hz .....	63
40. Response Motion for $f = 4.5$ Hz .....	63

## NOMENCLATURE

$a_{cg}$	linear acceleration of the center of gravity of each rod, in/sec <sup>2</sup> .
$d$	diameter of the cross-section of the rod, in.
$f_A, f_B$	driving forces acting on points A and B, lbs.
$f_c$	characteristic frequency of the system, Hz.
$f_{nb}$	natural frequency of the driving mechanism (cantilever beam), Hz.
$g$	acceleration due to gravity, in/sec <sup>2</sup> .
$l$	length of cantilever beam, in.
$l_1, l_2$	length of upper and lower elastic members
$m$	mass at the end of the beam, lb sec <sup>2</sup> /in.
$m_b$	mass of the beam, lb sec <sup>2</sup> /in.
$n$	number of rods
$t$	time, sec.
$y_L$	maximum deflection of cantilever beam, in.
$A$	area of the cross-section of the rod, in <sup>2</sup> .
$E$	elastic modulus of the beam material, lb/in <sup>2</sup> .
$F_A, F_B$	amplitude of driving force on points A and B, lbs.
$F_{RA}, F_{RB}$	rotational reaction forces on A and B, lbs.
$F_{TA}, F_{TB}$	translational reaction forces on A and B, lbs.
$I$	moment of inertia of the rods with respect to a vertical axis passing through the center of gravity, in. <sup>4</sup> .



$I_b$	moment of inertia of the cross-section of the beam, in. <sup>4</sup> .
$K_b$	elastic equivalent spring constant of a cantilever beam, lb/in.
$L$	length of each rod, in.
$R_A, R_B$	restoring forces on A and B, lb.
$T$	tension on first and last upper and lower elastic members, excluding that due to rod weights, lbs.
$T_b$	kinetic energy of the cantilever beam, lb-in.
$T_I$	inertial reaction torque, lb-in.
$V_b$	potential energy of the cantilever beam, lb-in.
$W$	weight of each rod, lb.
$X_A, X_B$	displacements of points A and B, in.
$\ddot{X}_A, \ddot{X}_B$	linear acceleration of points A and B, in/sec <sup>2</sup> .
$\bar{X}_A, \bar{X}_B$	amplitudes displacements of points A and B, in.
$\alpha_{AB}$	angular acceleration of the rod AB, rad/sec <sup>2</sup> .
$\omega$	driving frequency rad/sec.
$\omega_c$	characteristic angular frequency of the system, rad/sec.
$\omega_{nb}$	natural frequency of the cantilever beam, rad/sec.
$\phi$	angle of rotation of the rod with respect to its longitudinal rest position axis, rad.
$\rho$	specific weight of the material of the rod, lb/in <sup>3</sup> .
$\theta_A, \theta_B$	angle of rotation of the upper and lower elastic members at points A and B, rad.
$\theta'_A, \theta'_B$	

## SUMMARY

This thesis is concerned with the dynamic response of a vibrational system which consists of a chain of coupled rods secured to a lower and an upper frame using elastic members. This chain, called a series of bifilar pendulums, receives an external disturbance at one end in the form of an harmonical excitation.

The present study gives a mathematical model for the system, gives the solution of the equations of motion, and discusses results derived from such solutions. The motion response of the chain was studied by varying two significant parameters. One of these parameters is a function of the geometry of the rods, while the other is a function of the ratio of the driving frequency to the characteristic frequency of the system.

When these parameters were changed, the motion response changed significantly, especially when the values of the external driving frequency were about the same as that of the characteristic frequency of the system.

An experimental model was also built. This model was demonstrated to be successful in demonstrating the different responses of the system, which are in accord with the theoretical solution.

## CHAPTER I

### INTRODUCTION

The present work is concerned with the dynamic response of a vibrational mechanism consisting of a chain of coupled bifilar pendulums fixed to two frames, an upper and a lower frame, by means of long springs. The springs are fixed to the chain, one at each joint. The mechanism vibrates under the action of an external harmonic excitation at one end of the chain. The other end is free.

The physical parameters of the system, such as weight of the elements, tension on the springs, and shape and moment of inertia of each pendulum govern the magnitude of the characteristic frequency of the system. If one changes the magnitude of the driving frequency from slightly below the characteristic frequency to above its value the manner in which the chain vibrates changes significantly.

In order to study these changes, the author has devised a mathematical model for the mechanism and has constructed a prototype for the system whose physical properties are as close to the theoretical model as possible.

With use of the theoretical model, it was possible to predict the behavior of the system. The resulting numerical values were very useful in the design of the prototype as well as in the interpretation of the experimental results.

In the design of the prototype many factors were considered, involving cost of fabrication, ease of handling and operation, objec-

tivity in the results, ease of fabrication, etc. The actual construction was carried out using facilities in the Mechanical Engineering School at the Georgia Institute of Technology.

The results obtained from the experiments with the prototype are definitely in accord with the theoretical predictions as regards gross motions, although detailed numerical comparisons were not feasible. The principal difficulties in this regard are due to the presence of friction in the actual model and to the absence of suitable equipment for making measurements of the displacements of each joint of the chain. Neither simple vernier observations nor complex accelerometrics measurements were useful for this purpose.

The motivation for this work came from the reading of a non-published paper by Professor Takashi Nakada<sup>1</sup>, of the Tokyo Institute of Technology. This paper contains a short derivation establishing the dynamical properties of one bifilar pendulum which was used as a mechanical high-pass vibration filter.

Also helpful to the author was the reading of an article on dynamics of the bifilar pendulum by T. R. Kane<sup>2</sup> and Gan-Tai-Tseng of the Division of Engineering Mechanics at Stanford University.

## CHAPTER II

## MATHEMATICAL MODEL

Force Analysis

The system to be studied may be defined as a chain of  $n$  coupled rods fixed to a lower and an upper frame by elastic members. Both ends of the chain are free.

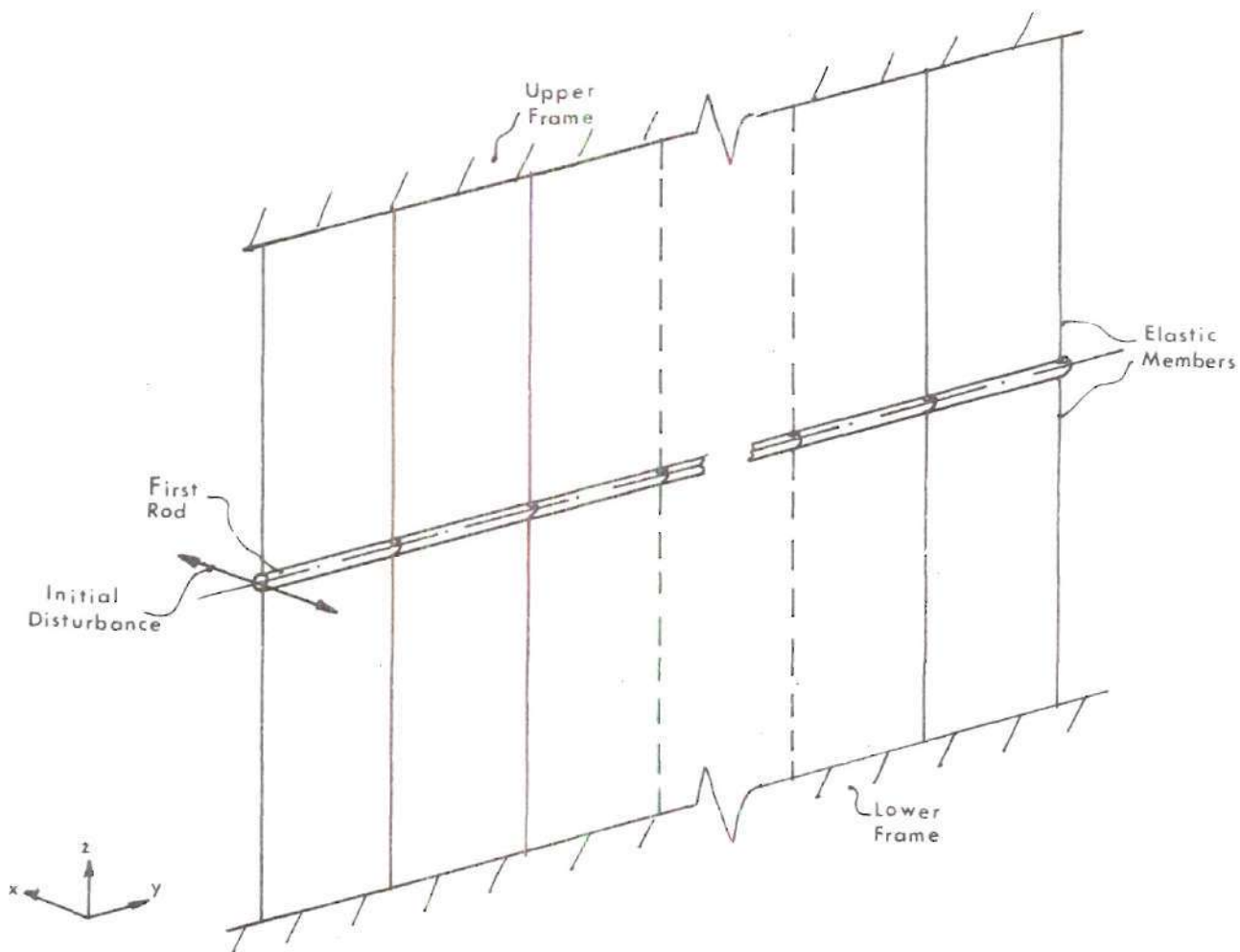


Figure 1. Schematic View of the System



In order to simplify the mathematical derivation , we initially limit our attention to just one rod, i.e. the first rod as shown on Fig. 1. However, the model for the study of this single rod implicitly incorporates the effects of all the rods of the chain.

If it is assumed that all rods have the same weight  $W$ , the difference in tensions of any intermediate elastic member in the upper row, and any corresponding member in the lower row is  $W$ . The first and the last elastic members will have upper minus lower tension difference  $\frac{W}{2}$ . If there are  $n$  rods, the total weight supported by the upper elastic members will be  $nW$ . The number of upper elastic members supporting the chain in Fig. 1 is the number of pendulum plus one. Thus, the total vertical force  $F$  on the chain is

$$[(n + 1) - 2]W + 2\left(\frac{W}{2}\right) = F$$

$$(n-1) W + W = F$$

$$nW = F$$

With this viewpoint, we say that the gravitational contribution to the tension in the upper elastic members is  $W/2, W, W, \dots, W/2$  as indicated in Fig. 2.

If in addition to the gravitational contribution to the tension each intermediate elastic member is assumed to have an additional tension  $2T$  while the first and last members have additional tension  $T$ , there will be a force distribution as shown on Fig. 3.

It is convenient to assume that instead of one upper elastic intermediate member at each intermediate joint with a tension  $2T+W$ ,

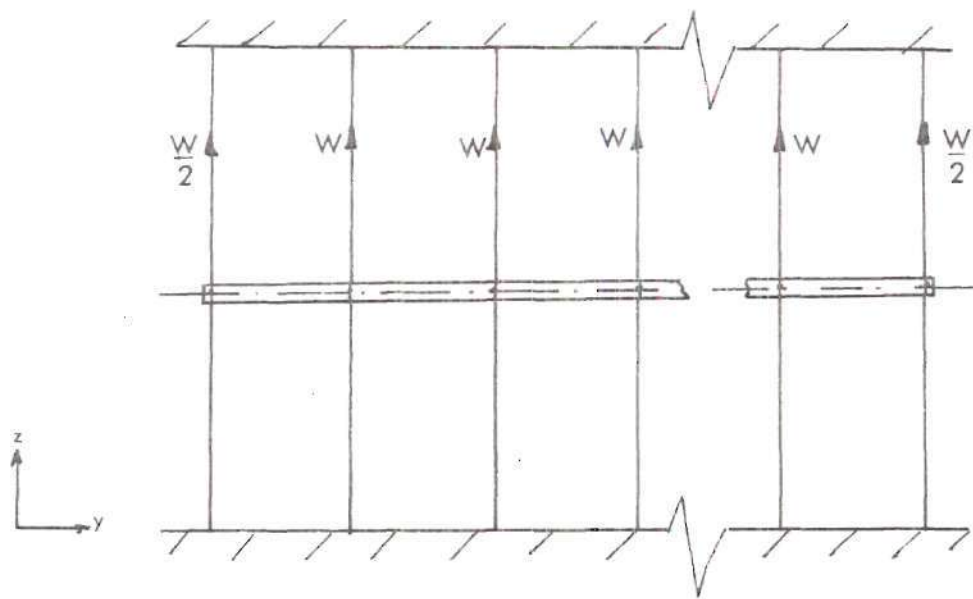


Figure 2. Force Distribution in the upper Elastic Members due only to Gravity. The Arrows Indicate the Forces Exerted on the Elastic Members by the upper Supports.

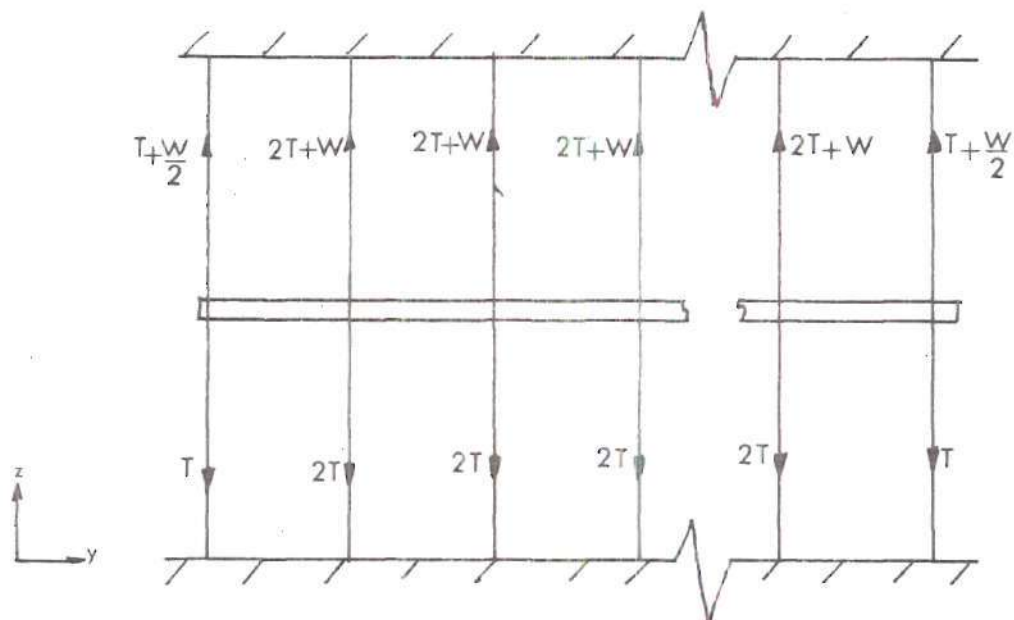


Figure 3. Force Distribution Including Gravitational and Tension Forces.

there are two elastic members present, each one with a force  $T + \frac{W}{2}$ . One of them is attached to the rod at the left of the joint, and the other is attached to the rod at the right of the joint, giving a force distribution as shown in Fig. 4.

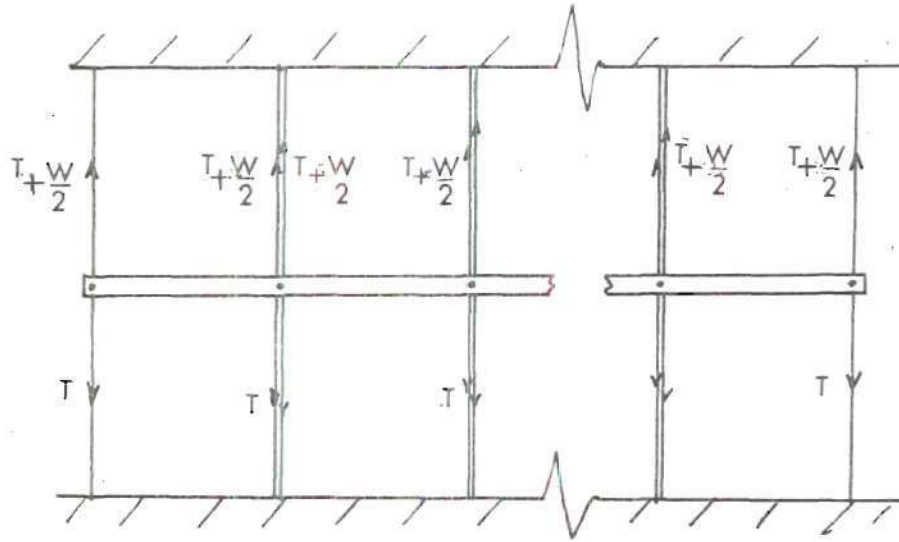


Figure 4. Final Force Distribution

Thus the model chosen for the mathematical derivation is one rod with weight  $W$ , length  $L$ , area  $A$  and moment of inertia  $I$ , fixed to a lower frame by an elastic member under the action of a tension  $T$ , and to an upper frame by a member under a tension  $T + \frac{W}{2}$ .

The upper and lower elastic members are taken to be  $l_1$  and  $l_2$  units long, respectively, as shown on Fig. 5.

We next consider the resultant motion of a single rod, under the action of an external harmonical excitation with a frequency  $\omega$ .

The presence of the excitation on the rod at the left can be represented as a force  $f_A$  acting normal to the longitudinal axis of the



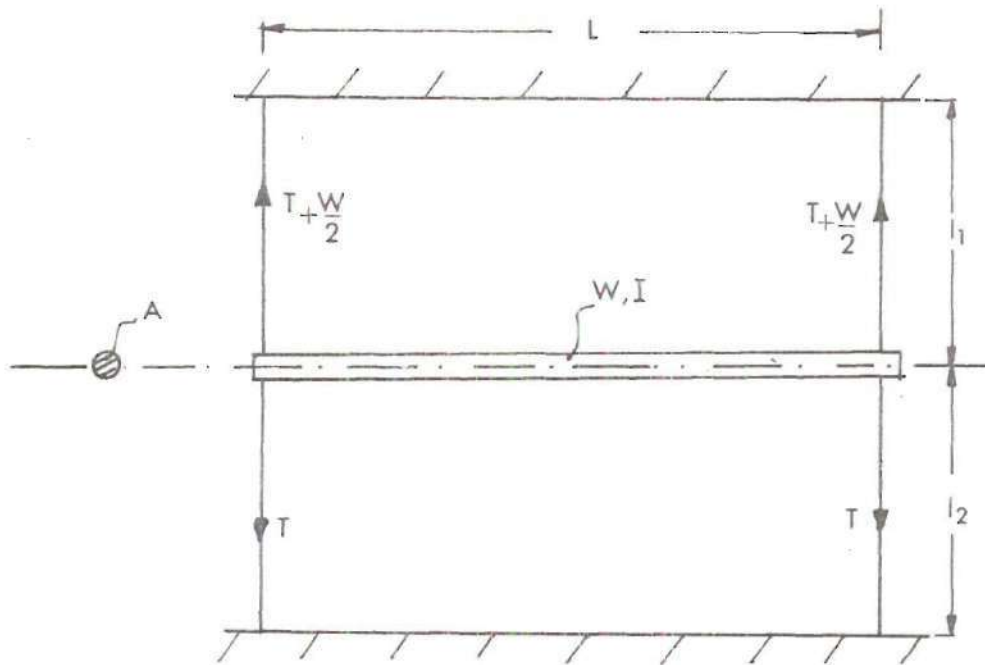


Figure 5. Selected Model for Derivation

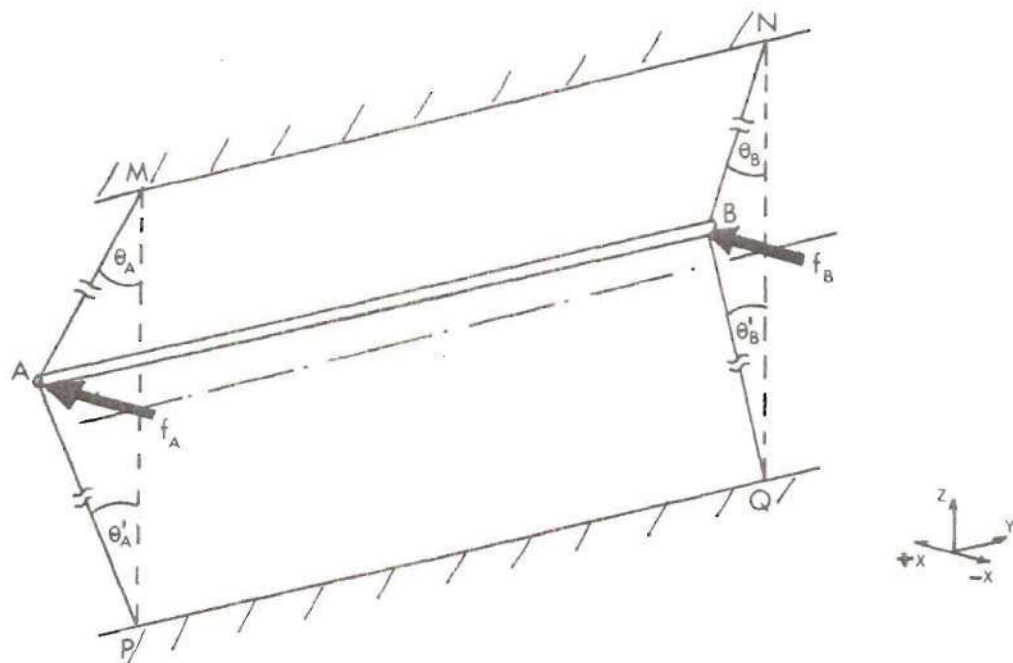


Figure 6. External Forces Acting on a Single Rod.

rod at the end A. Since the point B on the rod is jointed to the input terminal of the next element on the chain, a second force is acting on end B, and its value is taken as  $f_B$  with a sign sense opposite to that adopted for  $f_A$ , consistent with Newton's third law (see Fig. 6). A reaction force in the minus direction due to the next stage input terminal implies a positive force on the left end of the next rod, as shown in Fig. 7.

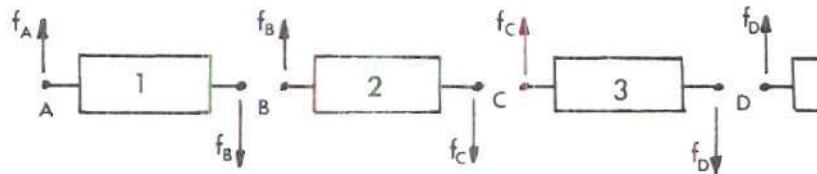


Figure 7. Internal Forces

For given angles of deflection of the elastic members from the vertical, such as  $\theta_A$  and  $\theta_B$  and  $\theta'_A$  and  $\theta'_B$ , due to the tensions in these members, there will be horizontal restoring forces  $R_A$  and  $R_B$ , acting on the rod. (See Fig. 8). It is assumed that the tensions in the elastic members are insignificantly increased due to stretching. Providing  $T$  is sufficiently large this would be an appropriate assumption. If one designates  $X_A$  and  $X_B$  as the displacements of the points A and B in the +X direction, the restoring force at point A will be:

$$R_A = \left(T + \frac{W}{2}\right) \sin \theta_A + T \sin \theta'_A$$

where

$$\sin \theta_A = \frac{X_A}{l_1}, \quad \sin \theta'_A = \frac{X_A}{l_2}$$

thus

$$R_A = \left(T + \frac{W}{2}\right) \cdot \frac{X_A}{l_1} + T \cdot \frac{X_A}{l_2} = \left(\frac{T}{l_1} + \frac{T}{l_2} + \frac{W}{2l_1}\right) X_A$$

$$R_A = \left[ T\left(\frac{1}{l_1} + \frac{1}{l_2}\right) + \frac{W}{2l_1} \right] X_A \quad (1)$$

The restoring force at point B will therefore be:

$$R_B = \left(T + \frac{W}{2}\right) \sin \theta_B + T \sin \theta'_B$$

where

$$\sin \theta_B = \frac{X_B}{l_1}, \quad \sin \theta'_B = \frac{X_B}{l_2}$$

It accordingly follows that

$$R_B = \left(T + \frac{W}{2}\right) \frac{X_B}{l_1} + T \frac{X_B}{l_2} = \left(\frac{T}{l_1} + \frac{T}{l_2} + \frac{W}{2l_1}\right) X_B$$

$$R_B = \left[ T\left(\frac{1}{l_1} + \frac{1}{l_2}\right) + \frac{W}{2l_1} \right] X_B \quad (2)$$

Due to the translational acceleration of rod AB one can, in the sense of one's writing Newton's second law as a static force balance, conceive of an inertial reaction force acting on the body AB. This force,  $F_T$ , according to Newton's second law of motion is

$$F_T = \frac{W}{g} \cdot a_{cg}$$

where

$W$  = weight of the rod

$g$  = gravity acceleration

$a_{cg}$  = acceleration of the center of gravity on body AB

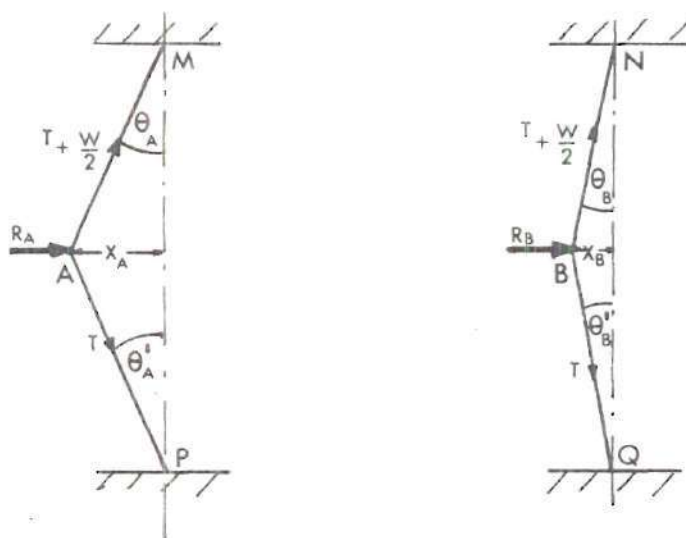


Figure 8. Restoring Forces

Since the center of gravity is in the center of the rod, one can consider the force  $F_T$  as divided into two forces  $F_{TA}$  and  $F_{TB}$ , each one equal to one-half the value of  $F_T$ , and acting at points A and B, respectively (See Fig. 9.) This follows since the rod is symmetrical with respect to an axis passing through its middle point and thus the center of gravity will be located at this point. As indicated in Fig. 9, it is possible to say that the displacement of the center of gravity is equal to one-half the value of  $X_A$  plus  $X_B$ . Then, the acceleration of this point is

$$a_{cg} = \frac{d^2}{dt^2} \left( \frac{X_A + X_B}{2} \right) = \frac{1}{2} \left( \frac{d^2 X_A}{dt^2} + \frac{d^2 X_B}{dt^2} \right)$$

One accordingly identifies reaction forces  $F_{TA}$  and  $F_{TB}$  as

$$F_{TA} = \frac{1}{2} \left( \frac{W}{g} \right) \cdot \frac{1}{2} \left( \frac{d^2 X_A}{dt^2} + \frac{d^2 X_B}{dt^2} \right) = F_{TB}$$

or

$$F_{TA} = \frac{W}{4g} (\ddot{X}_A + \ddot{X}_B) \quad (3)$$

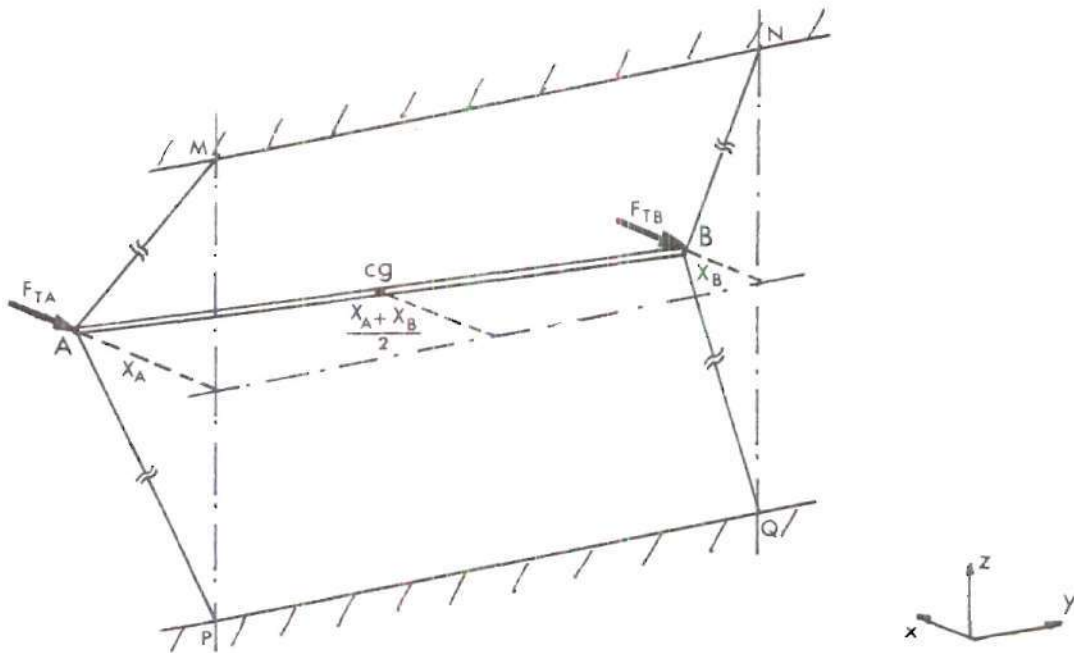


Figure 9. Inertial Translational Reaction Forces

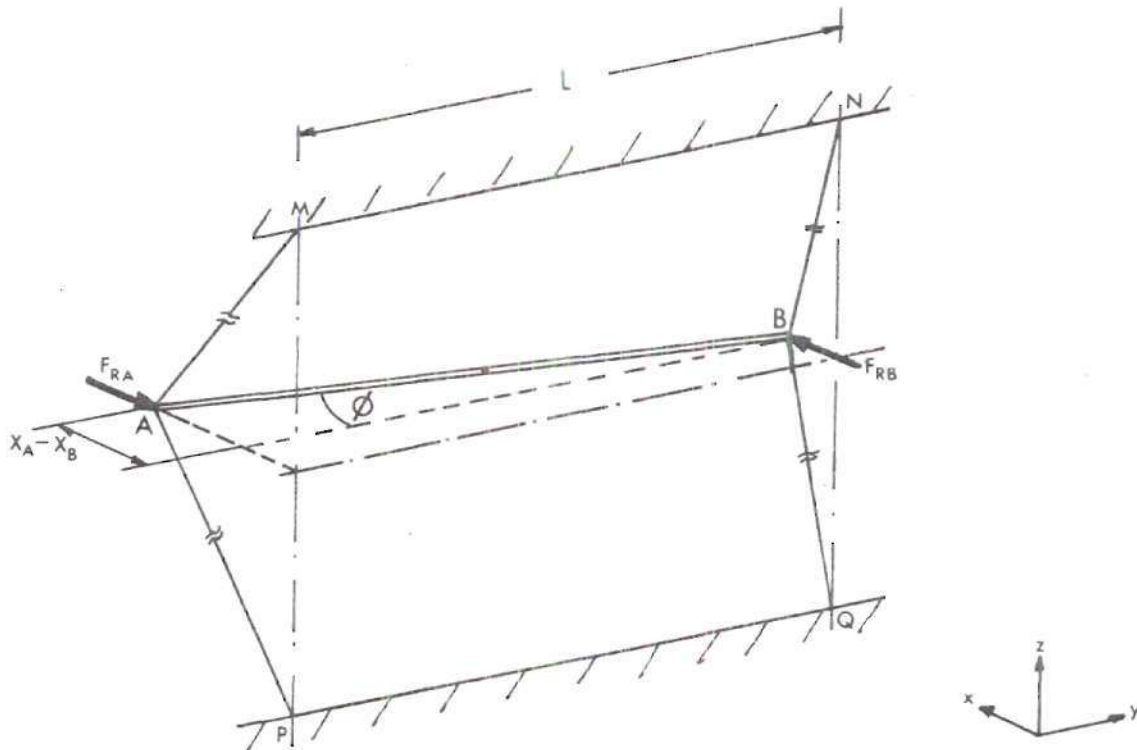


Figure 10. Inertial Rotational Reaction Forces

$$F_{TB} = \frac{W}{4g} (\ddot{X}_A + \ddot{X}_B) \quad (4)$$

Due to the rotational motion of the rod AB, about the vertical axis through the center of gravity of the rod's weight, there is an inertial reaction torque,  $T_I$ , acting on the body equal to the product of the moment of inertia  $I$  of the body and its angular acceleration  $\alpha_{AB}$ .

$$T_I = I \cdot \alpha_{AB}$$

This torque may be expressed as two forces, each of the same value but with different direction acting on each end of the rod. The torque will be equal to the product of this force with the length of the element.  
or

$$T_I = F_{R_{A \text{ or } B}} \cdot L$$

from which one identifies

$$F_{R_A} = - F_{R_B} = \frac{T_I}{L} = \frac{I}{L} \cdot \alpha_{AB}$$

The angle  $\phi$  of rotation of the body in the horizontal plane with respect to its original rest position may be approximated by the value of its tangent for small angles or rotation, i.e.

$$\phi \cong \tan \phi = \frac{\frac{1}{2} (X_A - X_B)}{\frac{L}{2}} = \frac{X_A - X_B}{L}$$

The angular acceleration of the body is accordingly

$$\alpha_{AB} = \frac{d^2 \phi}{dt^2} = \frac{d^2}{dt^2} \left( \frac{X_A - X_B}{L} \right) = \frac{1}{L} (\ddot{X}_A - \ddot{X}_B)$$

and one therefore identifies

$$F_{RA} = \frac{I}{L^2} (\ddot{X}_A - \ddot{X}_B) \quad (5)$$

$$F_{RB} = \frac{I}{L^2} (\ddot{X}_B - \ddot{X}_A) \quad (6)$$

### Equations of Motion

All of the component forces discussed above are horizontal forces acting on the two ends of the rod. A complete diagram of these forces is presented in Fig. 11

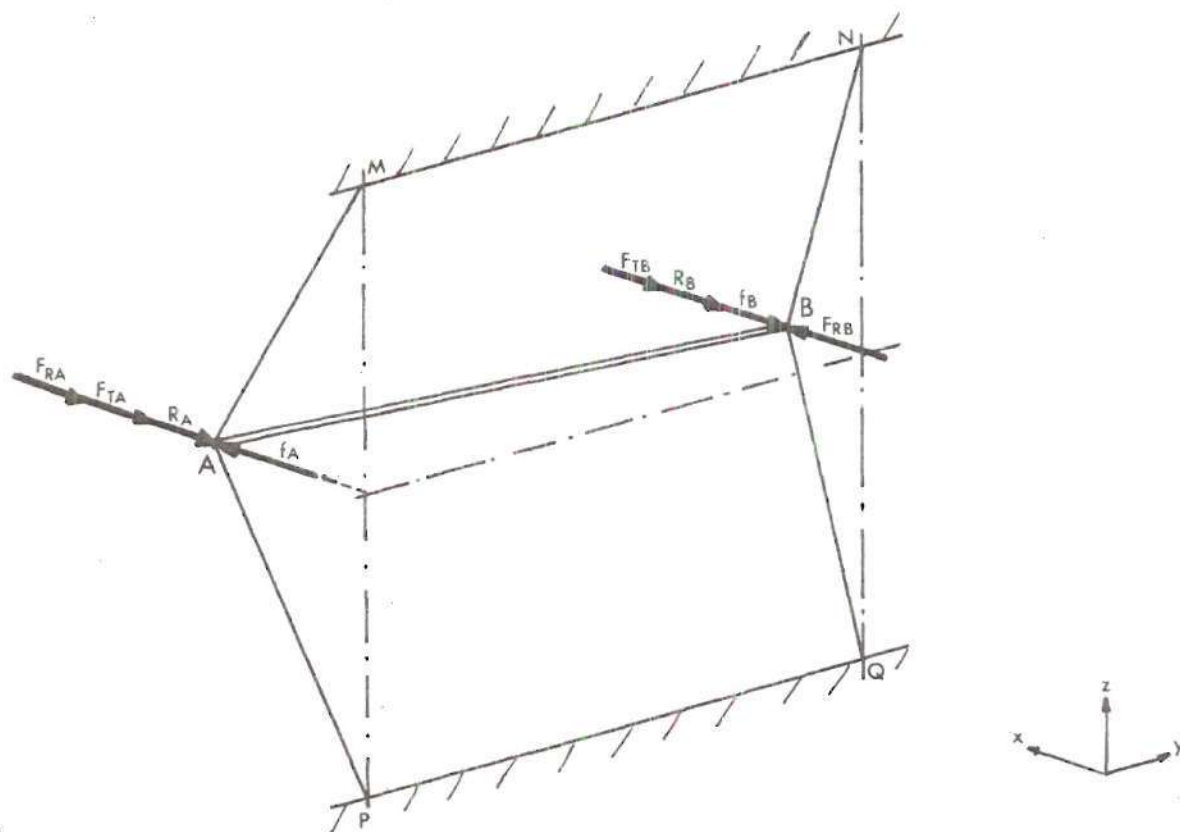


Figure 11. Forces in the Horizontal Direction Acting on a Single Rod.



Newton's second law with the inertial force convention implies that the net sum of all such forces in the +X direction should be zero. Furthermore, the net torque, including inertial torques should be zero. These two conditions are equivalent to saying that the net force acting at either end point should be zero. Thus, for point A, one has

$$\Sigma F_A = 0$$

$$F_A - R_A - F_{TA} - F_{RA} = 0$$

or

$$F_A - \left[ T \left( \frac{1}{l_1} + \frac{1}{l_2} \right) + \frac{W}{2l_1} \right] X_A = \frac{W}{4g} (\ddot{X}_A + \ddot{X}_B) + \frac{I}{L^2} (\ddot{X}_A - \ddot{X}_B) \quad (7)$$

while for point B, one has

$$\Sigma F_B = 0$$

$$F_B + R_B + F_{TB} + F_{RB} = 0$$

or

$$F_B + \left[ T \left( \frac{1}{l_1} + \frac{1}{l_2} \right) + \frac{W}{2l_1} \right] X_B = - \frac{W}{4g} (\ddot{X}_A + \ddot{X}_B) - \frac{I}{L^2} (\ddot{X}_B - \ddot{X}_A)$$

or

$$F_B + \left[ T \left( \frac{1}{l_1} + \frac{1}{l_2} \right) + \frac{W}{2l_1} \right] X_B = - \left[ \frac{W}{4g} (\ddot{X}_A + \ddot{X}_B) - \frac{I}{L^2} (\ddot{X}_A - \ddot{X}_B) \right] \quad (8)$$



these may be summarized as

$$f_A = \left( \frac{W}{4g} + \frac{I}{L^2} \right) \ddot{X}_A + \left[ T \left( \frac{1}{l_1} + \frac{1}{l_2} \right) + \frac{W}{2l_1} \right] \ddot{X}_B +$$

$$\left( \frac{W}{4g} - \frac{I}{L^2} \right) \ddot{X}_B \quad (9)$$

$$-f_B = \left( \frac{W}{4g} - \frac{I}{L^2} \right) \ddot{X}_A + \left[ T \left( \frac{1}{l_1} + \frac{1}{l_2} \right) + \frac{W}{2l_1} \right] \ddot{X}_B +$$

$$\left( \frac{W}{4g} + \frac{I}{L^2} \right) \ddot{X}_B \quad (10)$$

The values for  $W$ ,  $g$ ,  $I$ ,  $L$ ,  $T$ ,  $l_1$  and  $l_2$  are constant parameters for any given model. For this reason, it is convenient to make the following substitutions:

$$M = \frac{W}{4g} + \frac{I}{L^2}$$

$$N = \frac{W}{4g} - \frac{I}{L^2}$$

$$K = \left[ T \left( \frac{1}{l_1} + \frac{1}{l_2} \right) + \frac{W}{2l_1} \right]$$

Substituting these new constants  $M$ ,  $N$  and  $K$  into equations (9) and (10), one obtains

$$f_A = M \ddot{X}_A + K \ddot{X}_A + N \ddot{X}_B \quad (11)$$

$$-f_B = N \ddot{X}_A + K \ddot{X}_B + M \ddot{X}_B \quad (12)$$

If the external force applied to the assembly is an oscillatory function, the steady state displacement of the ends,  $X_A$  and  $X_B$ , of any rod along with the internal forces  $f_A$  and  $f_B$  may be expressed as the real parts of quantities having time dependency  $e^{i\omega t}$ , i.e.

$$X_A = \bar{X}_A e^{i\omega t} ; X_B = \bar{X}_B e^{i\omega t}$$

$$f_A = F_A e^{i\omega t} ; f_B = F_B e^{i\omega t}$$

where

$$\bar{X}_A, \bar{X}_B = \text{complex amplitude of points A and B}$$

$$F_A, F_B = \text{complex amplitudes of forces acting on A and B}$$

$$\omega = \text{angular frequency of oscillation}$$

It accordingly follows that

$$\ddot{X}_A = -\omega^2 \bar{X}_A e^{i\omega t}$$

$$\ddot{X}_B = -\omega^2 \bar{X}_B e^{i\omega t}$$

Substituting these values into Eq. (11), one obtains

$$F_A e^{i\omega t} = -M\omega^2 \bar{X}_A e^{i\omega t} + K\bar{X}_A e^{i\omega t} - N\omega^2 \bar{X}_B e^{i\omega t}$$

or

$$F_A = (-M\omega^2 + K) \bar{X}_A - N\omega^2 \bar{X}_B \quad (13)$$

Similarly, from Eq. (12), one obtains

$$-F_B e^{i\omega t} = -N\omega^2 \bar{x}_A e^{i\omega t} + K \bar{x}_B e^{i\omega t} - M\omega^2 \bar{x}_B e^{i\omega t}$$

or

$$-F_B = -N\omega^2 \bar{x}_A + (-M\omega^2 + K) \bar{x}_B \quad (14)$$

If one next solves Eq. (14) for  $\bar{x}_A$ , he obtains

$$\bar{x}_A = \frac{(-M\omega^2 + K)}{N\omega^2} \bar{x}_B + \frac{1}{N\omega^2} F_B \quad (15)$$

which, when substituted into Eq. (13), yields

$$F_A = (-M\omega^2 + K) \left[ \frac{(-M\omega^2 + K)}{N\omega^2} \bar{x}_B + \frac{1}{N\omega^2} F_B \right] - N\omega^2 \bar{x}_B$$

this then simplifies to

$$F_A = \left[ \frac{(M\omega^2 + K)(-M\omega^2 + K)}{N\omega^2} - N\omega^2 \right] \bar{x}_B + \frac{(-M\omega^2 + K)}{N\omega^2} F_B$$

or

$$F_A = \left[ \frac{(M^2 - N^2)\omega^4 - 2KM\omega^2 + K^2}{N\omega^2} \right] \bar{x}_B + \frac{(-M\omega^2 + K)}{N\omega^2} F_B \quad (16)$$

The above equation may also be written in the matrix form

$$\begin{bmatrix} \overline{X}_A \\ F_A \end{bmatrix} = \begin{bmatrix} \frac{(-M\omega^2 + K)}{N\omega^2} & \frac{1}{N\omega^2} \\ \frac{(M^2 - N^2)\omega^4 - sKM\omega^2 + K^2}{N\omega^2} & \frac{-M\omega^2 + K}{N\omega^2} \end{bmatrix} \begin{bmatrix} \overline{X}_B \\ F_B \end{bmatrix} \quad (17)$$

Alternately, if one makes the substitution

$$A = \frac{-M\omega^2 + K}{N\omega^2} \quad (18)$$

$$B = \frac{1}{N\omega^2} \quad (19)$$

$$C = \frac{(M^2 - N^2)\omega^4 - sKM\omega^2 + K^2}{N\omega^2} \quad (20)$$

$$D = \frac{-M\omega^2 + K}{N\omega^2} = A \quad (21)$$

the above may be written in the form

$$\begin{bmatrix} \overline{X}_A \\ F_A \end{bmatrix} = \begin{bmatrix} A & B \\ C & D \end{bmatrix} \begin{bmatrix} \overline{X}_B \\ F_B \end{bmatrix} \quad (22)$$

#### Application of the Equation of Motion to a Chain of Rods

The model of principal interest is a chain of coupled rods and we now have the equation of motion for one single rod. However, these

results may be used to analyze the motion of the enter chain, as is schematically shown in Fig. 12.

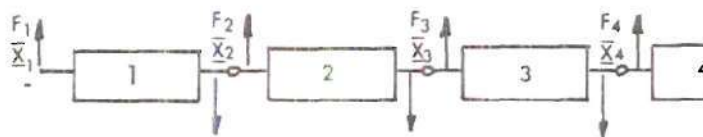


Figure 12. Interactions of the Chain

one has, for example, for the first rod, the equation

$$\begin{bmatrix} \bar{X}_1 \\ F_1 \end{bmatrix} = \begin{bmatrix} A & B \\ C & D \end{bmatrix} \begin{bmatrix} \bar{X}_2 \\ F_2 \end{bmatrix} \quad (22)$$

while for the second rod, one has

$$\begin{bmatrix} \bar{X}_2 \\ F_2 \end{bmatrix} = \begin{bmatrix} A & B \\ C & D \end{bmatrix} \begin{bmatrix} \bar{X}_3 \\ F_3 \end{bmatrix} \quad (23)$$

so one can express displacement and force at 1 in terms of displacement and force at 3 by the equation

$$\begin{bmatrix} \bar{X}_1 \\ F_1 \end{bmatrix} = \begin{bmatrix} A & B \\ C & D \end{bmatrix} \begin{bmatrix} A & B \\ C & D \end{bmatrix} \begin{bmatrix} \bar{X}_3 \\ F_3 \end{bmatrix}$$

or

$$\begin{bmatrix} \bar{X}_1 \\ F_1 \end{bmatrix} = \begin{bmatrix} A & B \\ C & D \end{bmatrix}^2 \begin{bmatrix} \bar{X}_3 \\ F_3 \end{bmatrix} \quad (24)$$

similarly

$$\begin{bmatrix} X_1 \\ F_1 \end{bmatrix} = \begin{bmatrix} A & B \\ C & D \end{bmatrix}^3 \begin{bmatrix} X_4 \\ F_4 \end{bmatrix} \quad (25)$$

or for a system consisting of n such rods, one has

$$\begin{bmatrix} \bar{X}_1 \\ F_1 \end{bmatrix} = \begin{bmatrix} A & B \\ C & D \end{bmatrix} \begin{bmatrix} \bar{X}_{n+1} \\ F_{n+1} \end{bmatrix} \quad (26)$$

the above is the general form of the equation of oscillatory motion for the proposed system. Some convenient interpretations are possible for the matrix  $[A, B, C, D]$  which appears in the above equations. Let us first note that Eqs. (11) and (12) may alternately be written as

$$\ddot{MX}_A + KX_A = f_A - N\ddot{X}_B \quad (11')$$

$$\ddot{MX}_B + KX_B = -f_B - N\ddot{X}_A \quad (12')$$

The form of these suggests that one define a characteristic frequency

$\omega_c$  as

$$\omega_c = \sqrt{\frac{K}{M}}$$

which serves as a convenient reference frequency for the system. The ratio of the driving frequency to  $\omega_c$  would accordingly appear to be a convenient dimensionless parameter, which we here term  $\delta$ , i.e.

$$\delta = \frac{\omega}{\omega_c}$$

another convenient dimensionless quantity is ratio  $\Psi$  of the two constants  $N$  and  $M$ , i.e.

$$\Psi = \frac{N}{M}$$

In terms of these quantities, one may readily express the matrix elements in the following form

$$A = \frac{1 - \delta^2}{\delta^2 \Psi^2} \quad (18')$$

$$B = \frac{1}{K \delta^2 \Psi} \quad (19')$$

$$C = \frac{K}{\Psi} \left[ (1 - \Psi^2) \delta^2 - 2 + \frac{1}{\delta^2} \right] \quad (20')$$

$$D = A = \frac{1 - \delta^2}{\delta^2 \Psi} \quad (21')$$

In terms of these identification, the Eq. (26) becomes

$$\begin{bmatrix} \bar{X}_1 \\ \frac{F_1}{K} \end{bmatrix} = \begin{bmatrix} \frac{1 - \delta^2}{\delta^2 \Psi} & \frac{1}{\delta^2 \Psi} \\ \frac{1}{\delta^2 \Psi} \left[ (1 - \Psi^2) \delta^4 - 2\delta^2 - 1 \right] & \frac{1 - \delta^2}{\delta^2 \Psi} \end{bmatrix} \begin{bmatrix} \bar{X}_{n+1} \\ \frac{F_{n+1}}{K} \end{bmatrix} \quad (27)$$

or

$$\begin{bmatrix} \bar{X}_1 \\ \frac{F_1}{K} \end{bmatrix} = \left[ \frac{1}{\delta^2 \Psi} \right]^n \begin{bmatrix} 1 - \delta^2 & 1 \\ \left[ (1 - \Psi^2) \delta^4 - 2\delta^2 + 1 \right] & 1 - \delta^2 \end{bmatrix} \begin{bmatrix} \bar{X}_{n+1} \\ \frac{F_{n+1}}{K} \end{bmatrix} \quad (28)$$

Since the left end of the chain is considered to be free there is no force at this end so

$$F_{n+1} = 0$$

this then gives us the following form for Eq. (27)

$$\begin{bmatrix} \bar{X}_1 \\ \frac{F_1}{K} \end{bmatrix} \begin{bmatrix} \frac{1 - \delta^2}{\delta^2 \Psi} & \frac{1}{\delta^2 \Psi} \\ \frac{1}{\delta^2 \Psi} & \left[ (1 - \Psi^2) \delta^4 - 2\delta^2 + 1 \right] \frac{1 - \delta^2}{\delta^2 \Psi} \end{bmatrix}^n \begin{bmatrix} \bar{X}_{n+1} \\ 0 \end{bmatrix} \quad (29)$$

The above Eq. (29) gives one a simple way for calculating the relative displacements of each joint of the chain, given any driving frequency. Such calculations are given in the next chapter.



### CHAPTER III

#### EXPERIMENTAL MODEL

This chapter presents two aspects of the design of the experimental model: (1) calculations based on the equations of motion previously derived. The input parameters are the physical constants for a given model, while the output contains the description of the predicted behavior of the model (2) The design and construction of the different parts of the model.

#### Calculations and Results

From Eq. (29) one may say that the displacement of any joint on a chain of  $n$  rods relative to the displacement at the input end is a function of just two numbers,  $\delta$  and  $\Psi$ . One may note that  $\Psi = N/M$  is in turn a function of the dimensionless quantity  $4gI/L^2W$  which represents the square of the ratio of a rod's radius of gyration to its half length  $L/2$ , i.e.

$$\Psi = \frac{1 - [r_G/(L/2)]^2}{1 + [r_G/(L/2)]^2}$$

The value of  $\delta$  is, as discussed previously, the ratio of the driving frequency  $\omega$  to the characteristic frequency  $\omega_c$ .

Physical Parameters. In the design of the model the following choices of parameters were made at the outset taking into account ease of fabrication and desired overall dimensions:

Tension on elastic members =  $T = 1$  lb.

Length of elastic members =  $l_1 = l_2 = 20$  in.

Weight of each rod = 0.5 lb.

Length of each rod = 4 in.

Values for  $\Psi$ . If one examines the relation,

$$\Psi = \frac{\frac{W}{4g} - \frac{I}{L^2}}{\frac{W}{4g} + \frac{I}{L^2}}$$

some limiting values may be predicted for  $\Psi$ . Since  $I$ ,  $W$ , and  $g$  are all positive the magnitude of the numerator must always be less than that of the denominator, so one can state

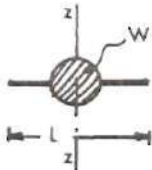
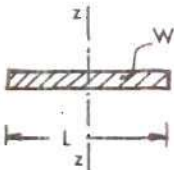
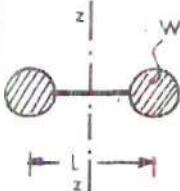
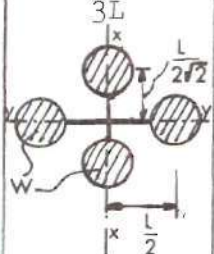
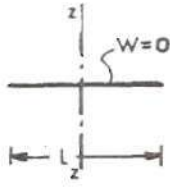
$$-1 < \Psi < 1$$

Calculations were performed for five different values of  $\Psi$ : 1,  $\frac{1}{2}$ , 0,  $-\frac{1}{2}$  and -1. Each of these values corresponds to a different value for  $I$ , and to a different corresponding shape for each of the rods. Table 1 summarizes the different alternatives.

Values for  $\delta$ . Exploratory calculations were performed for values of  $\delta$  ranging from 0.25 to 20.0. However, the results showed that significant changes occurred mainly in the range of values from 0.25 to 5.0, so, consequently, the chosen values for discussion are 0.5, 0.75, 1.0, 1.5, 2.0, 3.0, 5.0.

Another parameter intrinsic to the model is the number of rods in the chain. Our exploratory calculations seemed to indicate that 10 was sufficiently large to exhibit dynamical features expected for much longer chains and the fabrication complexities dictated that one not select an unrealistically large number.

Table 1. Values of  $\Psi$ ,  $I_{zz}$ , and Corresponding Rod Shape

$\Psi$	1	$\frac{1}{2}$	0	$-\frac{1}{2}$	-1
$I_{zz}$	0	$\frac{WL^2}{12g}$	$\frac{WL^2}{4g}$	$\frac{3WL^2}{4g}$	$\infty$
	(Lumped mass at center) 	(Cylindrical uniform rod) 	(Lumped masses at ends) 	Lumped masses on cross members at distance $\frac{3L}{2}$ 	(Radius of gyration infinite) 

As regards the computations per se let us note that Eq. (29) may alternately be written as

$$\begin{bmatrix} \bar{X}_1 \\ \frac{F_1}{K} \end{bmatrix} = \begin{bmatrix} \frac{1 - \delta^2}{\delta^2 \Psi} \\ -\frac{1}{\delta^2 \Psi} [(1 - \Psi^2)\delta^4 - 2\delta^2 + 1] \end{bmatrix} \begin{bmatrix} \frac{1}{\delta^2 \Psi} \\ \frac{1 - \delta^2}{\delta^2 \Psi} \end{bmatrix} \begin{bmatrix} \bar{X}_{11} \\ 0 \end{bmatrix} \quad (30)$$

or

$$\begin{bmatrix} \bar{X}_1 \\ \frac{F_1}{K} \end{bmatrix} = \begin{bmatrix} A' \\ C' \end{bmatrix} \begin{bmatrix} B' \\ D' \end{bmatrix} \begin{bmatrix} \bar{X}_{11} \\ 0 \end{bmatrix} \quad (31)$$

with obvious identifications for the symbols  $A', B', C', D' = A'$ . The matrix is alternately termed  $[P']$ , i.e.

$$[P'] = \begin{bmatrix} A' & B' \\ C' & D' \end{bmatrix}$$

The matrix  $[P']$  raised to the tenth power is also a  $2 \times 2$  matrix, which we here denote as  $[P'']$  with corresponding elements  $A'', B'', C''$  and  $D''$ , i.e.

$$\begin{bmatrix} A' & B' \\ C' & D' \end{bmatrix}^{10} = \begin{bmatrix} A'' & B'' \\ C'' & D'' \end{bmatrix} \quad (32)$$

thus, Eq. (31) may be written as

$$\begin{bmatrix} \bar{X}_1 \\ \frac{F_1}{K} \end{bmatrix} = \begin{bmatrix} A'' & B'' \\ C'' & D'' \end{bmatrix} \begin{bmatrix} \bar{X}_{11} \\ 0 \end{bmatrix} \quad (33)$$

or

$$\bar{X}_1 = A'' \bar{X}_{11} \quad (34)$$

$$\frac{F_1}{K} = C'' \bar{X}_{11} \quad (35)$$

from which one has

$$\frac{K\bar{X}_1}{F_1} = \frac{A''}{C''} \quad (36)$$

In order to calculate the relative displacements at intermediate joints on the chain, i. e. to determine the ratios  $\bar{X}_2/\bar{X}_1, \bar{X}_3/\bar{X}_1, \bar{X}_4/\bar{X}_1, \dots, \bar{X}_9/\bar{X}_1, \bar{X}_{10}/\bar{X}_1$ , Eq. (29) was reinterpreted.

$$\begin{bmatrix} \bar{X}_1 \\ \frac{F_1}{K} \end{bmatrix} = \begin{bmatrix} A' & B' \\ C' & D' \end{bmatrix}^i \begin{bmatrix} \bar{X}_i + 1 \\ \frac{F_{i+1}}{K} \end{bmatrix} \quad (37)$$

where  $i$  is any positive integer such that  $2 \leq i \leq 10$ . If one similarly defines matrix elements  $A'''$ ,  $B'''$ ,  $C'''$ ,  $D'''$

$$\begin{bmatrix} A' & B' \\ C' & D' \end{bmatrix}^i = \begin{bmatrix} A''' & B''' \\ C''' & D''' \end{bmatrix} \quad (38)$$

thus, Eq. (37) may be written as

$$\begin{bmatrix} \bar{X}_1 \\ \frac{F_1}{K} \end{bmatrix} = \begin{bmatrix} A''' & B''' \\ C''' & D''' \end{bmatrix} \begin{bmatrix} \bar{X}_i + 1 \\ \frac{F_{i+1}}{K} \end{bmatrix} \quad (39)$$

or, alternately, by the two equations

$$\bar{X}_1 = A''' \bar{X}_i + 1 + B''' \frac{F_{i+1}}{K} \quad (40)$$

$$\frac{F_1}{K} = C''' \bar{X}_i + 1 + D''' \frac{F_{i+1}}{K} \quad (41)$$

It follows from these in turn that

$$\frac{\bar{X}_1 - A''' \bar{X}_i + 1}{B'''} = \frac{\frac{F_1}{K} - C''' \bar{X}_i + 1}{D'''} \quad (42)$$

However, from Eq. (36), one has

$$\frac{F_1}{K} = \frac{C''}{A''} \bar{X}_1$$

so, Eq. (42) reduces to the following relation between  $\bar{X}_{i+1}$  and  $\bar{X}_1$

$$\frac{\bar{X}_1 - A''' \bar{X}_{i+1}}{B'''} = \frac{\frac{C''}{A''} \bar{X}_1 - C''' \bar{X}_{i+1}}{D'''} \quad (43)$$

or

$$\bar{X}_1 D''' - A''' D''' \bar{X}_{i+1} = \frac{C'' B'''}{A''} \bar{X}_1 - C''' B''' \bar{X}_{i+1} \quad (44)$$

If we divide this by  $\bar{X}_1$

$$D''' - A''' D''' \frac{\bar{X}_{i+1}}{\bar{X}_1} = \frac{C'' B'''}{A''} - C''' B''' \frac{\bar{X}_{i+1}}{\bar{X}_1} \quad (45)$$

and then solve the above resulting equation for  $\bar{X}_{i+1} / \bar{X}_1$ , we obtain

$$\frac{\bar{X}_{i+1}}{\bar{X}_1} = \frac{D''' - \frac{C'' B'''}{A''}}{A''' D''' - C''' B'''}$$

or simply

$$\frac{\bar{X}_{i+1}}{\bar{X}_1} = \frac{1}{A''} \frac{(A'' D''' - C'' B''')}{(A''' D''' - C''' B''')} \quad (46)$$

One may note that for the analytical model selected, there is no damping and, consequently the ratios  $\bar{X}_{i+1} / \bar{X}_1$  are all real. Also these ratios give the instantaneous ratio of the corresponding instantaneous displacement  $\bar{X}_{i+1}$  to  $\bar{X}_1$ .



All the matrices  $[P''']$  and  $[P'']$  were calculated by the use of a computer program, listed in Appendix 1, on the UNIVAC 1108, at the Georgia Institute of Technology. The corresponding values of the ratios  $\bar{X}_{i+1}/\bar{X}_1$  are given in Tables 3, 4, 5 and 6. Results for the case  $\Psi = 0$  are omitted. What actually would be predicted in this limiting case is that, regardless of the value of  $\bar{X}_1$ , the remaining  $\bar{X}_i$  for  $i = 2, 3, \dots, 11$  would all be identically zero. This should be apparent from Eqs. (28) and (46). Consequently, the case  $\Psi = 0$  is of relatively little interest.

Graphs of the chain's configuration based on the numerical values in Tables 3, 4, 5, and 6 are presented in Figs 13, 14, 15 and 16. These figures were used as a reference in the selection of the remaining physical parameters needed to completely specify the experimental model.

#### Design and Construction

As was previously pointed out, different values of  $\Psi$  imply different moments of inertia and different shapes of the individual rods. As indicated in Table 1, the most convenient shape for the rod from the stand point of fabrication is a cylindrical uniform rod. This reason plus the fact that there seems to be no spectacularly different type of response behavior for other values of  $\Psi$  suggested that we use cylindrical uniform rods in the construction of the model.

A detailed description of the design of the model is given below.

Rods.- Given that the shape, weight and length of the rods are already specified, the only questions to be considered are those involving selection of the diameter  $d$  of the rod and of the material. In regards to the latter taking into account cost and availability, possible choices

Table 2. Coefficients for Matrices [P']

$\Psi$	$\delta'$	0.25	0.5	0.75	1.0	1.5	2.0	3.0	5.0
1.0	A'	15.0	3.0	0.77	0.0	-0.55	-0.75	-0.88	-0.96
	B'	15.62	3.91	1.74	0.98	0.43	0.24	0.11	0.04
	C'	14.27	2.05	-0.23	-1.02	-1.59	-1.79	-1.93	-2.01
	D'	15.0	3.0	0.77	0.0	-0.55	-0.75	-0.88	-0.96
0.5	A'	30.0	6.0	1.55	0.0	-1.11	-1.50	-1.77	-1.92
	B'	31.35	7.82	3.48	1.95	0.87	0.48	0.22	0.08
	C'	28.73	4.46	0.41	-0.51	0.27	2.55	13.36	34.18
	D'	30.0	6.0	1.55	0.0	-1.11	-1.50	-1.77	-1.92
0	A'				$\infty$				
	B'				$\infty$				
	C'				0				
	D'				$\infty$				
-0.5	A'	-30.0	-6.0	-1.55	0.0	1.11	1.50	1.77	1.92
	B'	-31.35	-7.82	-3.48	-1.95	-0.87	-0.48	-0.22	-0.08
	C'	-28.73	-4.46	-0.41	0.51	-0.27	-2.55	-13.36	-34.18
	D'	-30.0	-6.0	-1.55	0.0	1.11	1.50	1.77	1.92
-1.0	A'	-15.0	-3.0	-0.77	0.0	0.55	0.75	0.88	0.96
	B'	-15.62	-3.91	-1.74	-0.98	-0.43	-0.24	-0.11	-0.04
	C'	-14.27	-2.05	0.23	1.02	1.59	1.79	1.93	2.01
	D'	-15.0	-3.0	-0.77	0.0	0.55	0.75	0.88	0.96



Table 3. Results for the case  $\gamma = 1.0$ 

$\delta$	$x_2/x_1$	$x_3/x_1$	$x_4/x_1$	$x_5/x_1$	$x_6/x_1$	$x_7/x_1$	$x_8/x_1$	$x_9/x_1$	$x_{10}/x_1$	$x_{11}/x_1$
0.25	--	--	--	--	--	--	--	--	--	--
0.5	$1.71 \times 10^{-1}$	$2.8 \times 10^{-2}$	$8.2 \times 10^{-4}$	$6.41 \times 10^{-5}$	$-7.74 \times 10^{-5}$	$5.57 \times 10^{-6}$	$7.11 \times 10^{-6}$	$1.37 \times 10^{-5}$	$-7.96 \times 10^{-7}$	$4.42 \times 10^{-8}$
0.75	1.18	0.797	0.102	-0.658	-1.18	-0.935	-0.538	0.240	0.982	1.25
1.0	0.0	-1.009	0	1.009	0	-1.02	0	1.02	0	-1.03
1.5	-0.898	0.001	0.903	-0.997	0.201	0.77	-1.05	0.414	0.6	-1.086
2.0	-1.652	1.459	-0.566	-0.633	1.50	-1.62	0.946	0.225	-1.26	1.69
3.0	8.24	-15.53	19.48	-18.96	14.45	-6.492	-2.791	11.52	-17.77	20.0
5.0	-0.87	0.675	-0.422	0.128	0.166	-0.447	0.696	-0.892	1.010	-1.052

Table 4. Results for the Case  $\gamma = 0.50$ 

$\delta$	$x_2/x_1$	$x_3/x_1$	$x_4/x_1$	$x_5/x_1$	$x_6/x_1$	$x_7/x_1$	$x_8/x_1$	$x_9/x_1$	$x_{10}/x_1$	$x_{11}/x_1$
0.25	--	--	--	--	--	--	--	--	--	--
0.5	$2.66 \times 10^{-1}$	$6.66 \times 10^{-1}$	2.02	1.12	$5.51 \times 10^{-1}$	$-5.99 \times 10^{-1}$	$1.8 \times 10^{-2}$	$-1.6 \times 10^{-2}$	$4.9 \times 10^{-3}$	$3.5 \times 10^{-11}$
0.75	$3.62 \times 10^{-1}$	$1.44 \times 10^{-1}$	$2.35 \times 10^{-1}$	$4.9 \times 10^{-3}$	$-2.4 \times 10^{-4}$	$1.0 \times 10^{-4}$	$1.1 \times 10^{-4}$	$5.7 \times 10^{-5}$	$-9.9 \times 10^{-5}$	$8.3 \times 10^{-5}$
1.0	0.0	-1.0	0.0	1.0	0	-1.0	0	1.01	0	-1.01
1.5	$-6.26 \times 10^{-1}$	$4.22 \times 10^{-1}$	$-2.78 \times 10^{-1}$	$1.37 \times 10^{-1}$	$-8.9 \times 10^{-2}$	$7.4 \times 10^{-2}$	$-9.5 \times 10^{-2}$	$2.3 \times 10^{-2}$	$9.4 \times 10^{-2}$	$1.8 \times 10^{-2}$
2.0	$-3.8 \times 10^{-1}$	$1.72 \times 10^{-2}$	$-4.93 \times 10^{-2}$	$2.67 \times 10^{-2}$	$-8.9 \times 10^{-3}$	$1.12 \times 10^{-3}$	$1.63 \times 10^{-3}$	$-1.35 \times 10^{-4}$	$-1.75 \times 10^{-4}$	$1.35 \times 10^{-4}$
3.0	$2.84 \times 10^{-1}$	$7.6 \times 10^{-2}$	$-2.3 \times 10^{-1}$	$-8.25 \times 10^{-3}$	$-5.12 \times 10^{-3}$	$1.21 \times 10^{-3}$	$8.22 \times 10^{-4}$	$2.87 \times 10^{-6}$	$-8.07 \times 10^{-6}$	$7.86 \times 10^{-6}$
5.0	$-2.8 \times 10^{-1}$	$7.6 \times 10^{-2}$	$-1.7 \times 10^{-2}$	$-9.35 \times 10^{-3}$	$-4.35 \times 10^{-3}$	$1.15 \times 10^{-3}$	$-7.11 \times 10^{-4}$	$1.73 \times 10^{-4}$	$8.23 \times 10^{-6}$	$6.22 \times 10^{-6}$

Table 5. Results for the Case  $\Psi = -0.50$ 

$\delta$	$x_2/x_1$	$x_3/x_1$	$x_4/x_1$	$x_5/x_1$	$x_6/x_1$	$x_7/x_1$	$x_8/x_1$	$x_9/x_1$	$x_{10}/x_1$	$x_{11}/x_1$
0.25	--	--	--	--	--	--	--	--	--	--
0.50	$-2.66 \times 10^{-1}$	$6.66 \times 10^{-1}$	-2.02	1.12	$-5.51 \times 10^{-1}$	$-5.99 \times 10^{-1}$	$-1.8 \times 10^{-2}$	$-1.6 \times 10^{-2}$	$-4.9 \times 10^{-3}$	$3.5 \times 10^{-11}$
0.75	$-3.62 \times 10^{-1}$	$1.44 \times 10^{-1}$	$-2.35 \times 10^{-1}$	$4.9 \times 10^{-3}$	$2.4 \times 10^{-4}$	$1.0 \times 10^{-4}$	$-1.1 \times 10^{-4}$	$5.7 \times 10^{-5}$	$9.9 \times 10^{-5}$	$8.3 \times 10^{-5}$
1.00	0	-1.0	0	1.0	0	-1.0	0	1.01	0	-1.01
1.5	$6.26 \times 10^{-1}$	$4.22 \times 10^{-1}$	$2.78 \times 10^{-1}$	$1.37 \times 10^{-1}$	$8.9 \times 10^{-2}$	$7.4 \times 10^{-2}$	$9.5 \times 10^{-2}$	$2.3 \times 10^{-2}$	$-9.4 \times 10^{-2}$	$1.8 \times 10^{-2}$
2.0	$3.8 \times 10^{-1}$	$1.72 \times 10^{-2}$	$4.93 \times 10^{-2}$	$2.67 \times 10^{-2}$	$8.9 \times 10^{-3}$	$1.12 \times 10^{-3}$	$-1.63 \times 10^{-3}$	$-1.35 \times 10^{-4}$	$1.75 \times 10^{-4}$	$1.35 \times 10^{-4}$
3.0	$2.84 \times 10^{-1}$	$7.6 \times 10^{-2}$	$2.3 \times 10^{-1}$	$-8.25 \times 10^{-3}$	$5.12 \times 10^{-3}$	$1.21 \times 10^{-3}$	$-8.22 \times 10^{-4}$	$2.81 \times 10^{-6}$	$8.07 \times 10^{-6}$	$7.86 \times 10^{-6}$
5.0	$2.8 \times 10^{-1}$	$7.6 \times 10^{-2}$	$1.7 \times 10^{-2}$	$-9.35 \times 10^{-3}$	$4.35 \times 10^{-3}$	$1.15 \times 10^{-3}$	$7.11 \times 10^{-4}$	$1.73 \times 10^{-4}$	$8.23 \times 10^{-6}$	$6.22 \times 10^{-6}$

Table 6. Results for the Case  $\gamma = -1.0$ 

$\delta$	$x_2/x_1$	$x_3/x_1$	$x_4/x_1$	$x_5/x_1$	$x_6/x_1$	$x_7/x_1$	$x_8/x_1$	$x_9/x_1$	$x_{10}/x_1$	$x_{11}/x_1$
0.25	--	--	--	--	--	--	--	--	--	--
0.5	$-1.71 \times 10^{-1}$	$2.8 \times 10^{-2}$	$-8.2 \times 10^{-4}$	$6.41 \times 10^{-5}$	$7.74 \times 10^{-5}$	$5.57 \times 10^{-6}$	$-7.11 \times 10^{-6}$	$1.37 \times 10^{-5}$	$7.96 \times 10^{-7}$	$4.42 \times 10^{-8}$
0.75	-1.18	0.797	-0.102	-0.658	1.18	-0.935	0.538	0.24	-0.982	1.25
1.0	0	-1.009	0	1.009	0	-1.02	0	1.02	0	-1.03
1.5	0.898	0.001	-0.903	0.997	-0.201	0.77	1.05	0.414	-0.60	-1.086
2.0	1.652	1.459	0.566	-0.633	-1.50	-1.62	-0.946	0.225	1.26	1.69
3.0	-8.24	-15.53	-19.48	-18.96	-14.45	-6.492	2.791	11.52	17.77	20.0
5.0	0.87	0.675	0.422	0.128	-0.166	-0.447	-0.696	-0.892	-1.01	-1.052

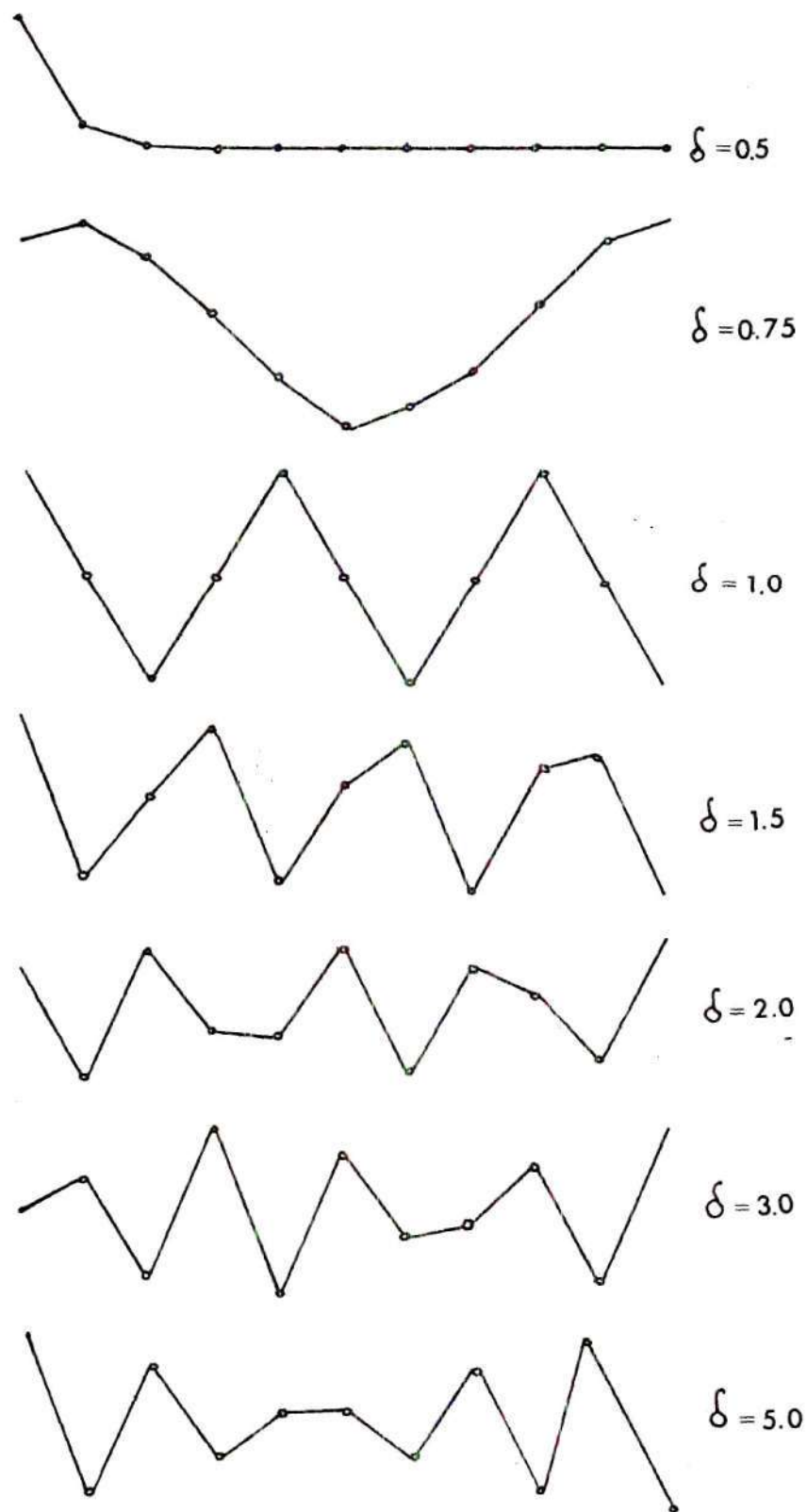


Figure 13. Chain Motion for  $\Psi = 1.0$

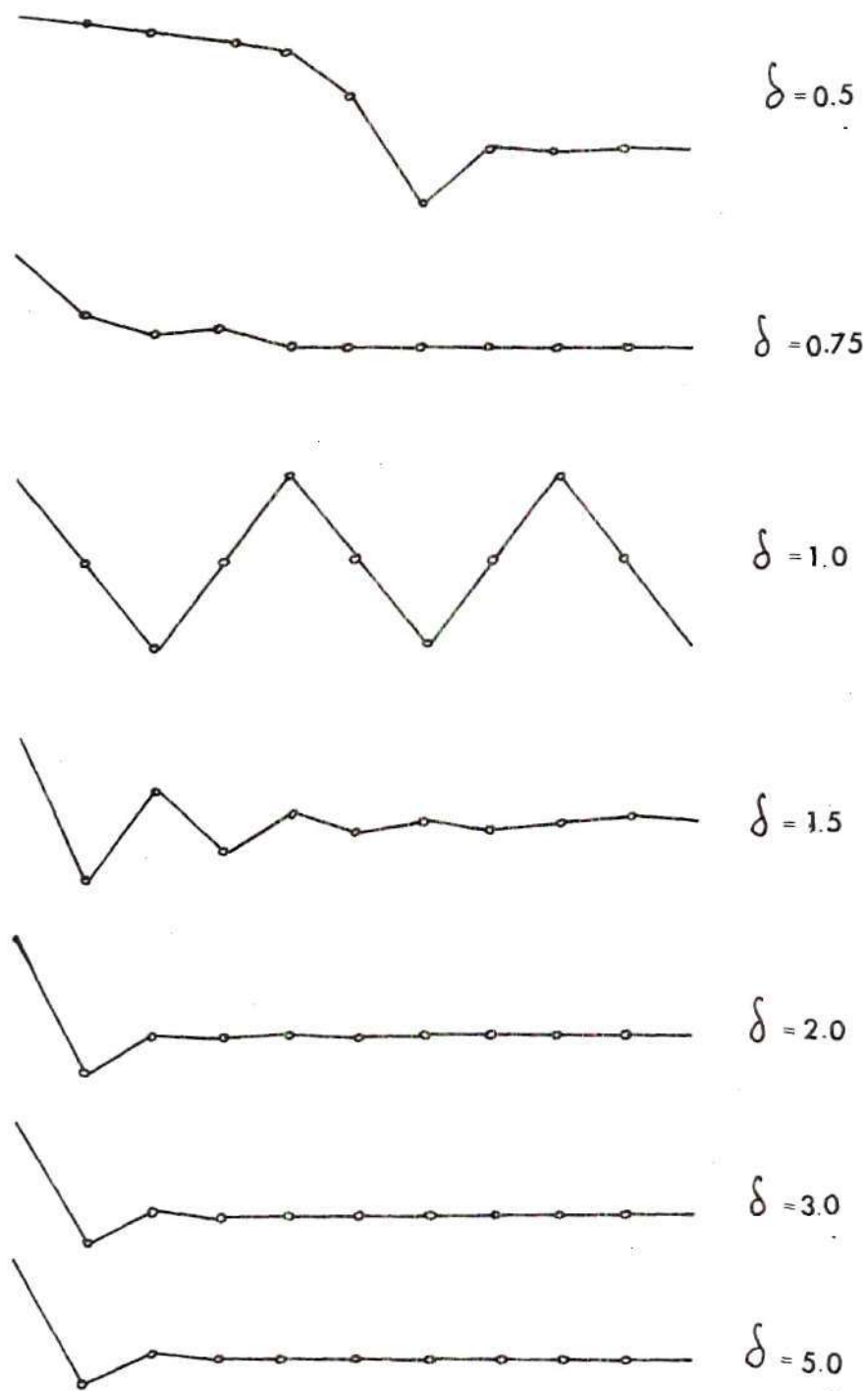


Figure 14. Chain Motion for  $\Psi = 0.5$

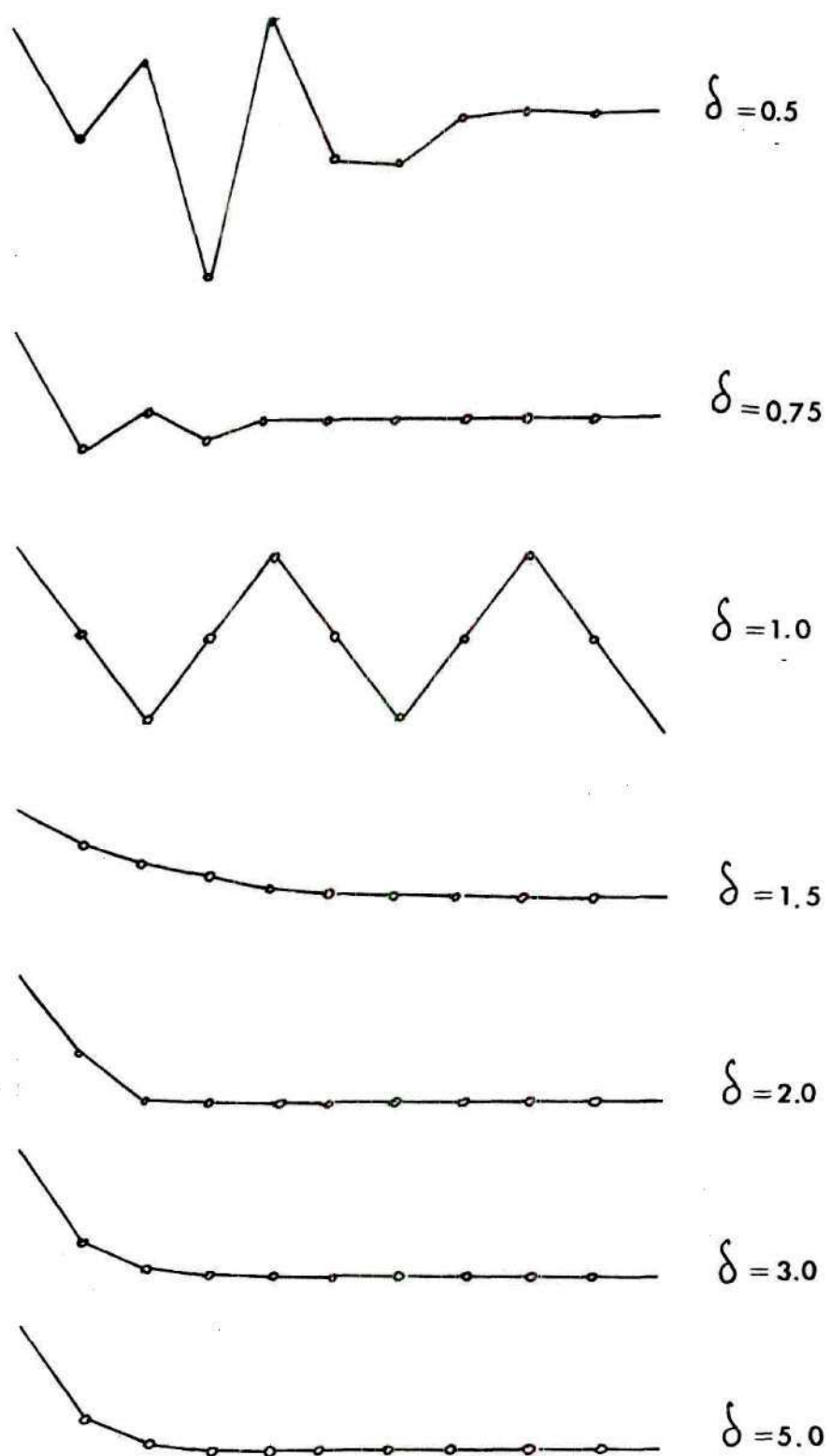


Figure 15. Chain Motion for  $\Psi = -0.5$



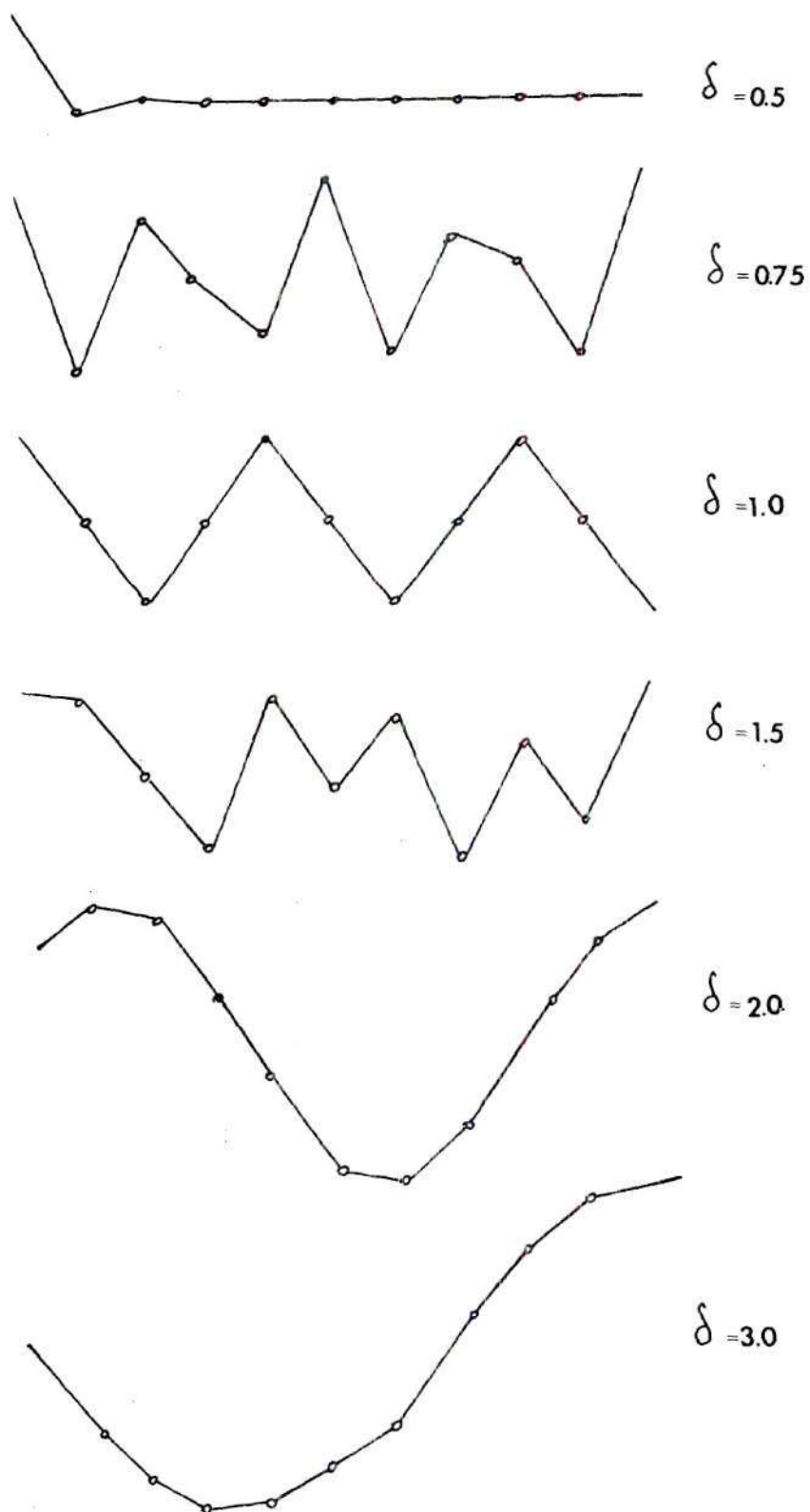


Figure 16. Chain Motion for  $\Psi = -1.0$

would be steel and aluminum. Steel was selected primarily because of its greater density. Since

$$W = \frac{\pi}{4} d^2 \cdot L \cdot \rho$$

where

$\rho$  = specific weight of the material

$d$  = diameter of the cross-section of the rod

$L$  = length of the rod



Figure 17. Geometry of the Rod

the diameter  $d$  would have to vary with  $\rho$  as

$$d = \sqrt{\frac{4W}{\pi \cdot L \cdot \rho}} \quad (48)$$

or, with the values  $W = 0.5$  lb,  $L = 4$  in; as

$$d = \sqrt{\frac{0.159}{\rho}} \quad (49)$$

if one substitutes here for  $\rho$  the specific weight for steel and aluminum respectively one finds

$$d_s = \sqrt{\frac{0.159}{\rho_s}} = \sqrt{\frac{0.159}{0.283}} = 0.75 \text{ in.} \quad (50)$$

$$d_a = \sqrt{\frac{0.159}{\rho_a}} = \sqrt{\frac{0.159}{0.1015}} = 1.26 \text{ in.} \quad (51)$$

Since a smaller size model would seem desirable, one prefers a smaller diameter on the rod. Also, the calculated diameter for the steel rod, 3/4 inch, is a standard commercial size for steel. Thus, we selected a 3/4 inch diameter steel rod. The moment of inertia for each rod would then be

$$I = \frac{Wl^2}{12g} = \frac{0.5 \text{ lb. } (4 \text{ in})^2}{12 \frac{(386 \text{ in})}{\text{sec}^2}} = 1.73 \times 10^{-3} \text{ lb in sec}^2 \quad (52)$$

Since the analytical model assumed each element on the chain to be pin jointed at its ends to adjacent elements, a cylindrical joint was designed to simulate this. (See Fig. 18.)

Finally, in order to attach the nominally vertical elastic members, to each joint, two eye-screws were attached at the two ends of each 3/8" bolt which served as a pin in the cylindrical joint (Fig. 18) connecting adjacent rods. This part is shown in Fig. 19.

In accord with the overall design specification of 10 rods total, 8 rods were constructed as indicated in Fig. 20 a, i.e, to accommodate pin joints at the two ends. The remaining two, the first and the last on the chain, (which are pinned only at one end) were constructed as indicated in Fig. 20 b.

Elastic Members. Several choices were considered in regard to this part of the design. Piano wire and screen door springs were two easily available possibilities. Because of the relatively low tension (one pound) desired and the constraint that this tension not change markedly with lateral rod deflections, the screen-door springs were selected in preference to the piano wire. These springs are commercially

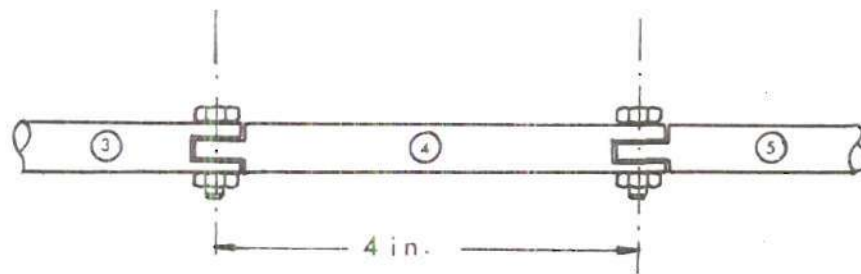


Figure 18a. Pinned Joints on the Chain

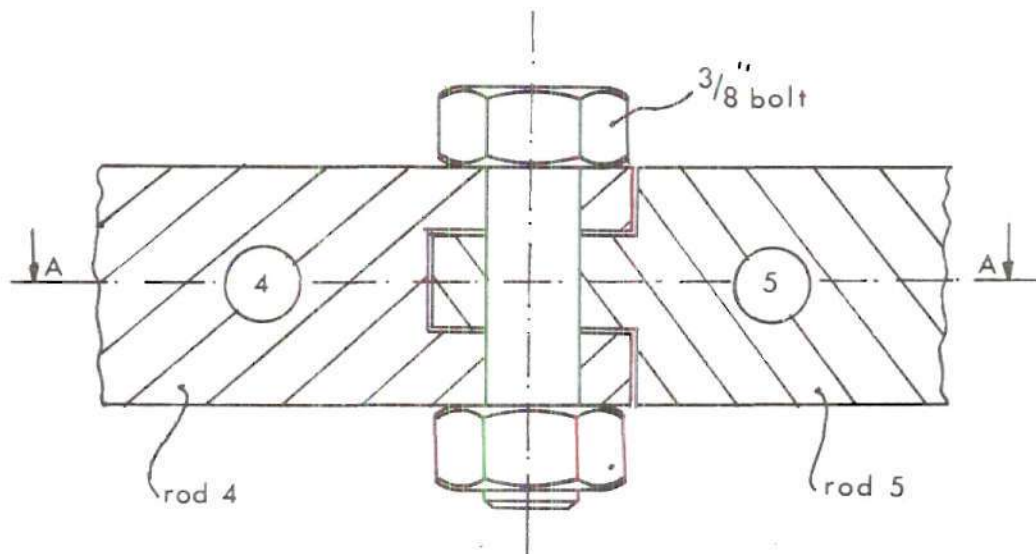


Figure 18b. Sectional view of the joint

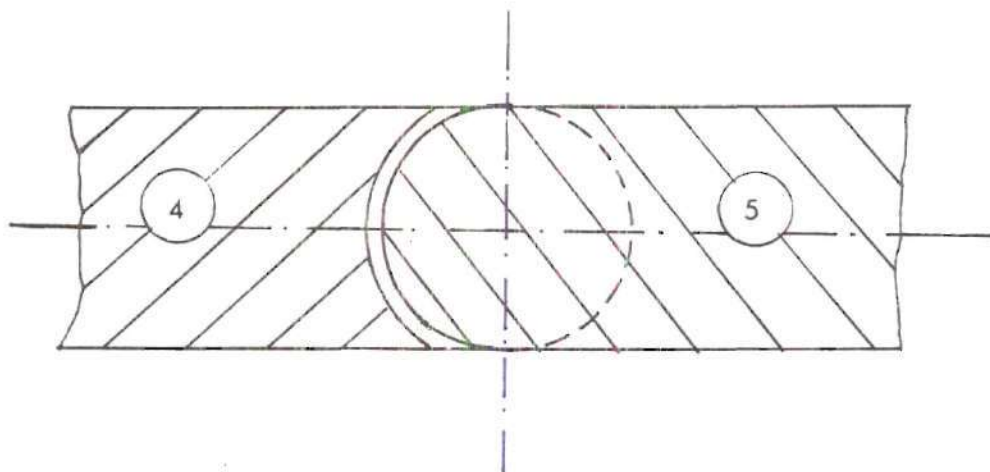


Figure 18c. Top View A-A

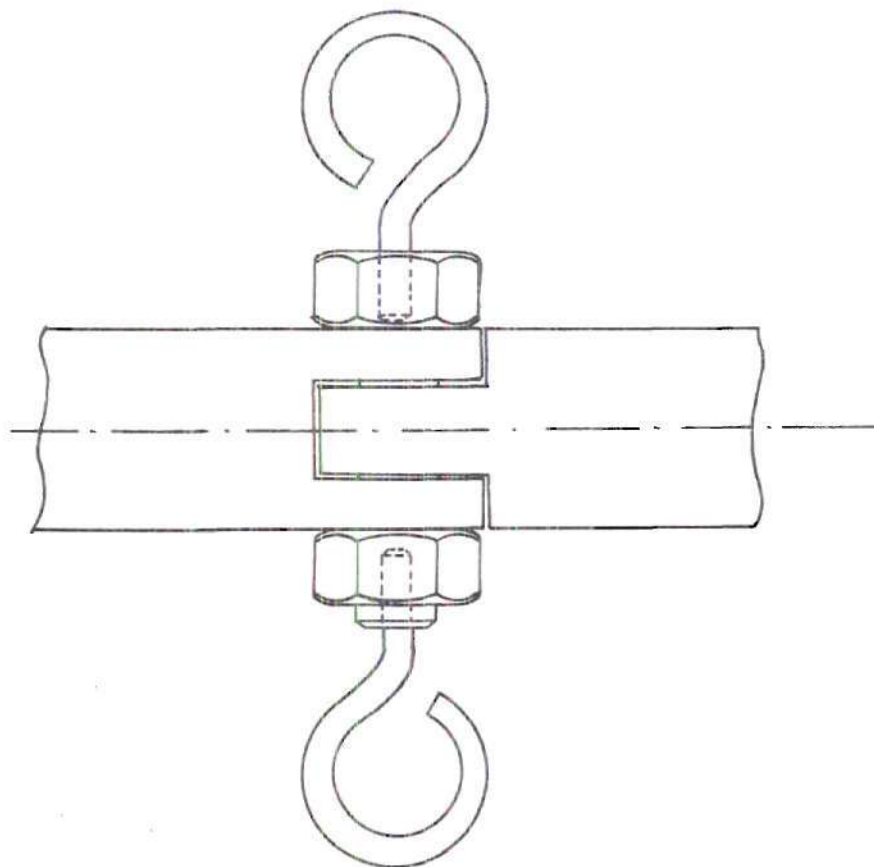


Figure 19. Eye-Screws at a Joint

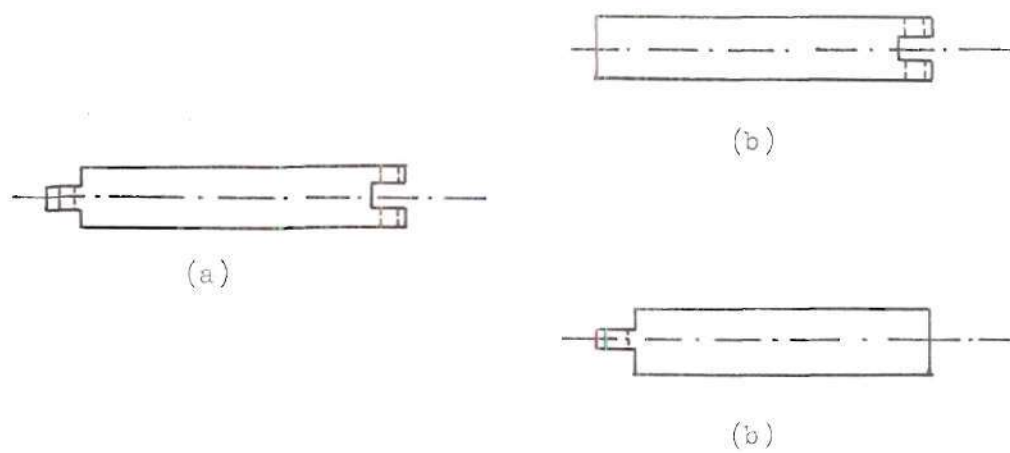


Figure 20 a) Intermediate Rods  
b) First and Last Rods

available and have an overall length of  $16\frac{1}{16}$  in., which is close to the 20 in. assumed in the calculations.

The spring constant of the door-spring is 1 lb. per  $\frac{1}{16}$  in. so tensions of  $2T+W$  or  $2T$ , respectively (were  $T = 1$  lb,  $W = \frac{1}{2}$  lb) would cause elongations of  $\frac{5}{32}$  and  $\frac{1}{8}$  in., Consequently, one would want the average elongations of upper and lower springs to be  $\frac{9}{64}$  in. In our model this average statical elongation was taken to be  $\frac{1}{16}$  in. corresponding to  $T = \frac{3}{8}$  lb. The average statical elongation for the four springs at the end was  $\frac{1}{32}$  in.

The loops at the ends of the springs were hooked onto eye-screws fixed to the chain and to the upper and lower frame as shown in Fig. 21.

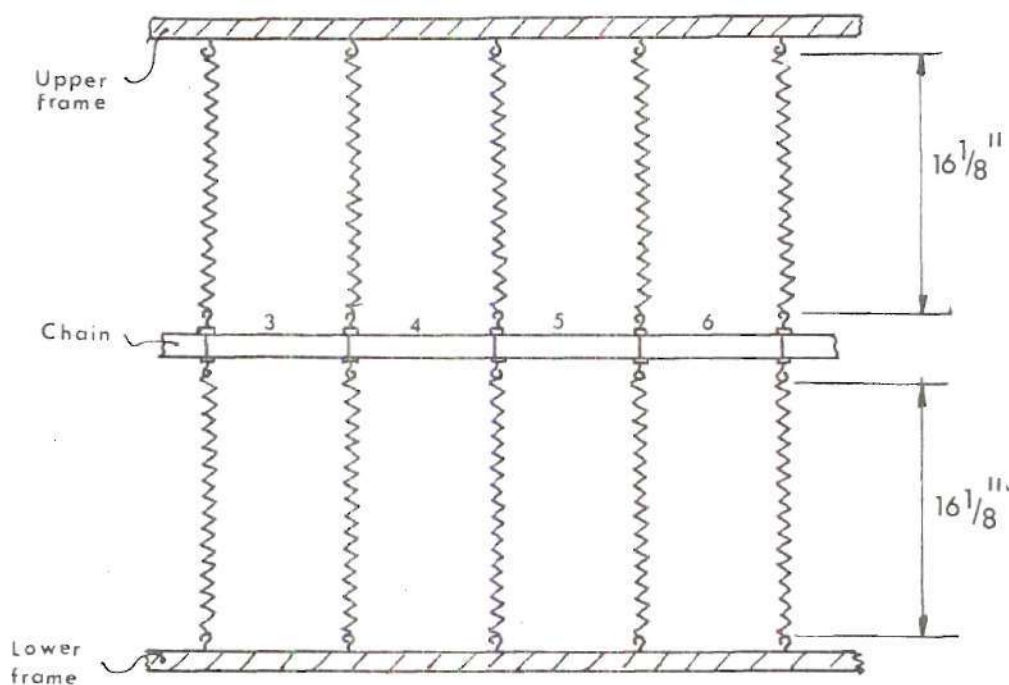


Figure 21. Elastic Members

External Driving Mechanism. A basic consideration in the design of this mechanism is the range of driving frequencies. The calculations presented here suggest that the significant changes in the motion of the chain occur at input frequencies with values in the vicinity of the characteristic frequency  $W_c$ , i . e. near

$$W_c = \sqrt{\frac{K}{M}} \quad (53)$$

where

$$K = \left[ T \left( \frac{1}{l_1} + \frac{1}{l_2} \right) + \frac{W}{2l_1} \right] \quad (54)$$

$$M = \frac{W}{4g} + \frac{I}{L^2} \quad (55)$$

the values of these quantities appropriate to the experimental model may be calculated by taken

$$T = \frac{3}{8} \text{ lb.}$$

$$l_1 = l_2 = 16 \frac{1}{8}''$$

$$L = 4''$$

The weight of each rod was determined by dividing the total weight of the chain (rods plus bolts and screws) by ten, giving

$$W = \frac{5.61}{10} = 0.561 \text{ lb.}$$

and

$$I = \frac{1}{12} \frac{WL^2}{g} = \frac{1}{12} \frac{(0.56)(16)}{386} = 1.93 \times 10^{-3} \text{ lbinsec}^2$$

There one has

$$K = \frac{3}{8} \left( \frac{1}{16.125} + \frac{1}{16.125} \right) + \frac{0.56}{2(16.125)} = 0.064 \frac{\text{lb}}{\text{in}}$$



$$M = \frac{0.56}{4 (386)} + \frac{1.93 \times 10^{-3}}{16} = 4.83 \times 10^{-4} \frac{\text{lb sec}^2}{\text{in}}$$

$$\omega_c = \sqrt{\frac{0.064 \text{ lb/in}}{4.83 \times 10^{-4} \text{ lbsec}^2/\text{in}}} = 13.25 \text{ sec}^{-2}$$

or

$$f_c = \frac{\omega_c}{2\pi} = \frac{13.25}{6.28} = 2.11 \text{ Hz}$$

For the design of the driving mechanism, frequencies ranging from  $0.5 f_c$  to  $1.5 f_c$  were desired. Thus the driving mechanism should be capable of driving the mechanism at frequencies between 1.06 Hz and 3.17 Hz. The automatic shaker available in the School of Mechanical Engineering was inappropriate for the purpose because it was designed for the 20 Hz to 2000 Hz range. Also a simple rod with a large mass at the end was considered but the necessary length to produce a harmonic vibration of 3.17 Hz was found to be 0.64 in which was far too small when compared with the size of the model.

The solution finally selected was a cantilever beam, with a mass at its end, whose length could be varied from 12.1 to 24.9 in. The natural vibration frequency could then be varied over the desired range of driving frequencies.

A brief discussion of the theory of this driving mechanism is given below (see Fig. 22).

If the deflection of the mass is denoted by  $y_L$ , then the kinetic energy of the system is given by

$$T_b = \frac{1}{2} m \dot{y}_L^2 + \frac{1}{2} m_b \dot{y}_L^2 \alpha \quad (56)$$

where  $\alpha$  is the average over length of the ratio of the square of the

beam's deflection to  $y_L^2$ . It is well known from the statical theory of beam deflections<sup>3</sup> that  $\alpha$  is very nearly equal to  $1/4$ . Similarly the potential energy may be taken as

$$V_b = \left(\frac{1}{2}\right) K_b y_L^2 \quad (57)$$

where  $K_b$  is the apparent spring constant of the beam when a static deflection force is applied at its end.

The conservation of energy thus implies that

$$\frac{d}{dt} (T_b + V_b) = m \dot{y}_L \ddot{y}_L + \frac{m_b}{4} \dot{y}_L \ddot{y}_L + K_b y_L \dot{y}_L = 0 \quad (58)$$

Dividing by  $\dot{y}_L$  then gives

$$\left(m + \frac{m_b}{4}\right) \ddot{y}_L + K_b y_L = 0 \quad (59)$$

which is the equation of motion for a system with natural frequency  $\omega_{nb}$ , the square of which is

$$\omega_{nb}^2 = \frac{K_b}{m + \frac{m_b}{4}} \quad (60)$$

The spring constant of the beam is calculated as follows. Consider a cantilever beam with a force applied at the end as in Fig. 23.

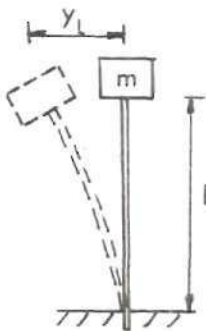


Figure 22.  
Cantilever with  
Mass at End

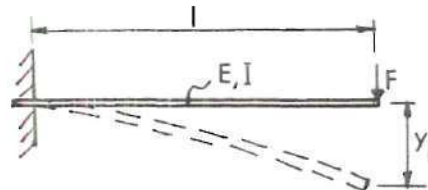


Figure 23. Deflection of a  
Cantilever Beam

A free-body diagram at any segment centered at a point  $x$  can be constructed as in Fig. 24.

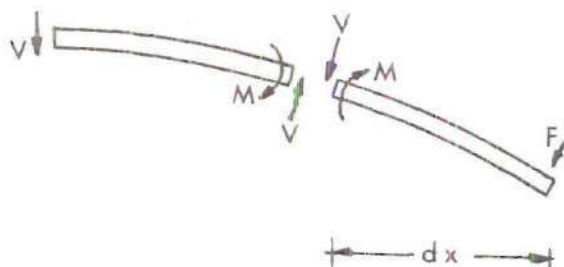


Figure 24. Force Analysis of a Cantilever Beam

The consequent application of the theory of beams gives

$$V = F \quad \text{and} \quad M = \int_x^l V \, dx$$

therefore

$$M = F (l - x)$$

It accordingly follows that

$$\frac{M}{EI_b} = \frac{d^2y}{dx^2} = \frac{F (l - x)}{EI_b} \quad (61)$$

where

$E$  = modulus of elasticity of the beam

$I_b$  = moment of inertia of cross-section of the beam

after integrating the above twice we have

$$\frac{F}{EI_b} \left( lx - \frac{x^2}{2} \right) = \frac{dy}{dx}$$

so

$$\frac{F}{EI_b} \left( \frac{1}{2}x^2 - \frac{x^3}{6} \right) = y$$

The boundary conditions are that  $y=dy/dx = 0$  at  $x = 0$ , while  $y = y_L$  at  $x = L$ , therefore

$$y_L = \frac{F}{EI_b} \left( \frac{1}{2}L^2 - \frac{1}{6}L^3 \right) = \frac{F}{EI_b} \frac{1}{3}L^3$$

If  $K_b$  is defined such that  $F = K_b y_L$ , then the apparent spring constant  $K_b$  is simply

$$K_b = \frac{F}{\frac{F}{EI_b} \frac{1}{3}L^3} = \frac{3EI_b}{L^3} \quad (62)$$

It then follows that the value for the natural frequency is

$$\omega_{nb}^2 = \frac{3EI_b}{L^3 \left( m + \frac{mb}{4} \right)} \quad (63)$$

It is possible to express the area moment of inertia of the beam as a function of the dimensions of the cross-section area. For the present case a rectangular section steel beam with a cross-sectional area  $\frac{1}{2}$ " x  $1/8$ ", is to be used. Its moment of inertia, referring to Fig. 25.

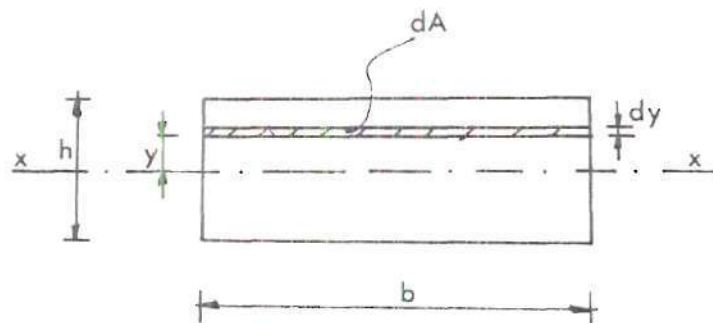


Figure 25. Moment of Inertia of the Beam Section

$$\begin{aligned}
 I_{b^{xx}} &= 2 \int_0^{h/2} y^2 dA = 2 \int_0^{h/2} y^2 b dy = 2b \int_0^{h/2} y^2 dy \\
 I_{b^{xx}} &= \frac{bh^3}{12} \\
 I_{b^{xx}} &= \frac{\frac{1}{2} \cdot \left(\frac{1}{8}\right)^3}{12} = \frac{1}{1.2 \times 2^{10}} \text{ in}^4 \quad (64)
 \end{aligned}$$

The mass of the beam can be also expressed as a function of the volume and the specific weight of the material by the formula

$$m_b = \frac{W_b}{g} = \frac{b h l \rho_{\text{steel}}}{g} \quad (65)$$

$$m_b = \frac{\frac{1}{2} \cdot \frac{1}{8} \cdot (0.28) \text{ l}}{g} = \frac{0.0175 \text{ l}}{g} \frac{\text{lb}}{\text{in sec}^2}$$

Thus, the natural frequency is

$$\omega_{nb}^2 = (2\pi f_{nb})^2 = 3 \cdot E \cdot \frac{1}{12 \times 2^{10}} \cdot \frac{1}{l^3} \cdot \frac{1}{\left(m + \frac{0.0175 \text{ l}}{4g}\right)}$$

The appropriate value for  $E_{\text{steel}}$  is  $30 \times 10^6 \text{ lb/in}^2$ , and if one assumes a value for  $m$  of  $\frac{4 \text{ lb}}{g}$  for the mass at the end, one has

$$4\pi^2 f_{nb}^2 = \frac{3 \cdot 30 \cdot 10^6}{12 \cdot 2^{10} \cdot \left(\frac{4}{386} + \frac{0.0175}{1544} \text{ l}\right) l^3}$$

The last equation may be reordered as follows:

$$0.0175 \text{ l}^4 + 16 \text{ l}^3 = 255 \cdot 10^3 \quad (66)$$

When the lower value of the range of frequencies desired i.e.  $f_{nb} = 1.06$  Hz, is substituted. The solution is

$$l = 24.9 \text{ in.}$$

Similarly, if the upper value is substituted,  $f_{nb} = 3.17$  Hz one has

$$0.0175 l^4 + 16 l^3 = 28.5 \cdot 10^3 \quad (67)$$

which gives

$$l = 12.1 \text{ in.}$$

Thus the desired design is a cantilever beam with a 4-lb weight at the end whose length can vary from 12.1 to 24.9 in. The designed mechanism is shown in Figs. 26a and 26b.

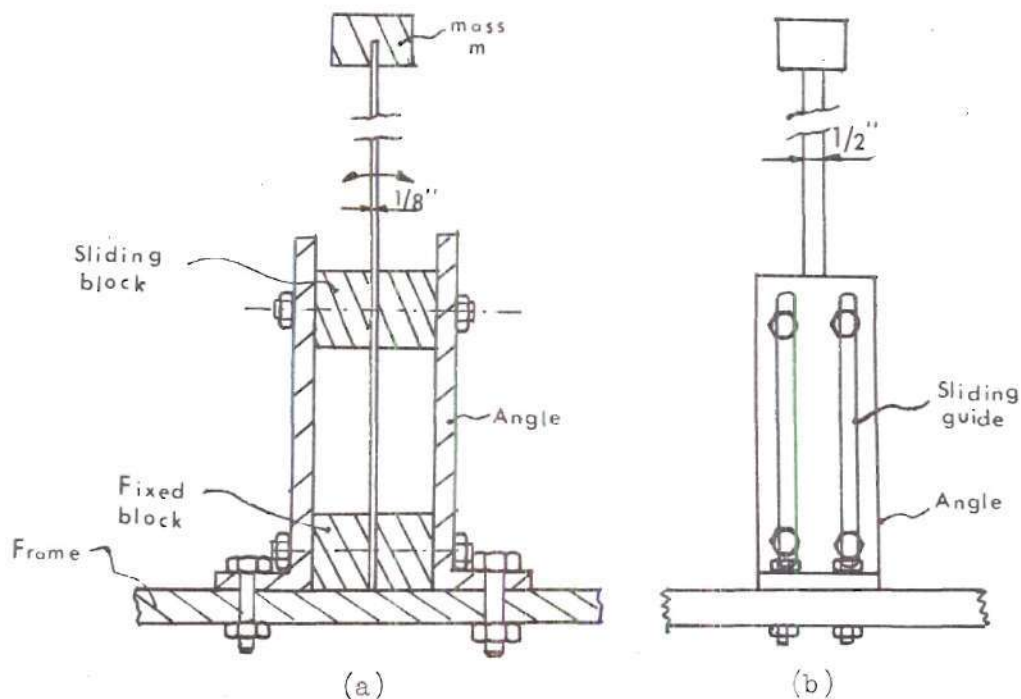


Figure 26. Driving Mechanism

- a) Middle Section Front View
- b) Side View



The driving mechanism is basically a beam fixed at one end to a non-moving block. There is another block which can be positioned at any point up to 10.5 inches from the upper face of the fixed block. With two bolts passing through the block, it is possible to secure it such that the beam is completely secured, giving another cantilever beam with a different length.

The mass at the end acts as an energy reservoir, the greater the amount of energy stored, the longer vibration time for the mechanism. An initial displacement must be given to the system and then the motion will continue for a considerable time period.

This mechanism is fastened to the chain by the small part shown in Fig. 27.

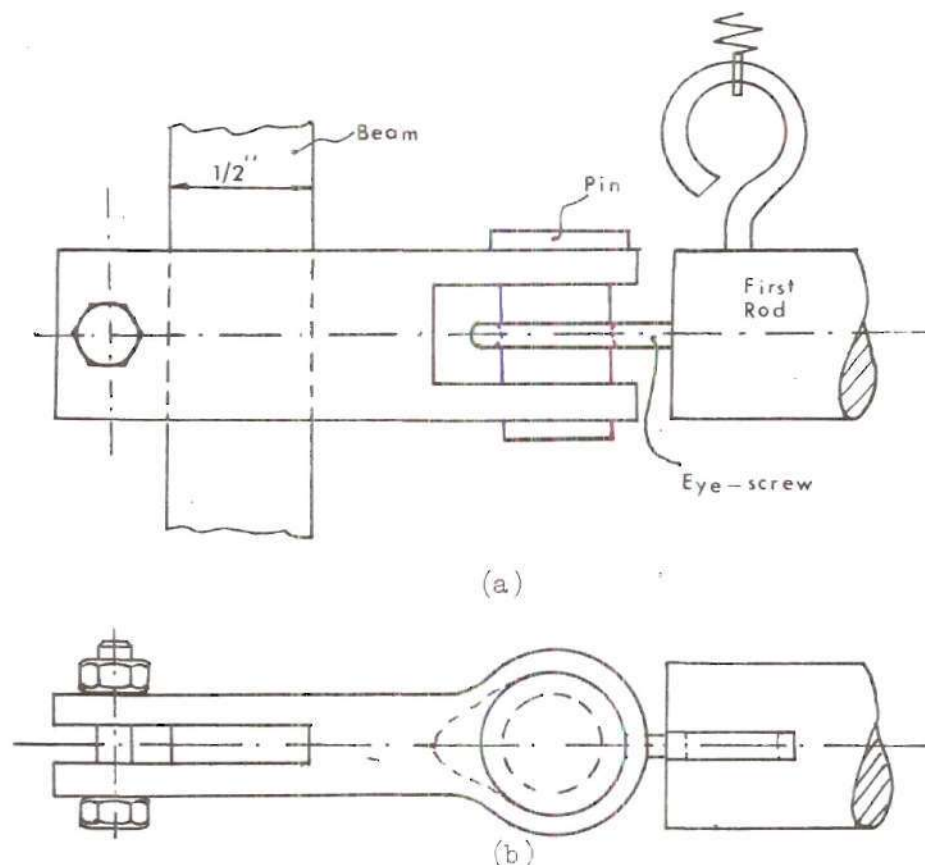


Figure 27. Beam-Rod Coupling  
 a) Front View  
 b) Top View



Frame. All the parts of the designed mechanism were put together within a wooden frame specially designed and built for this purpose. A schematic view of this frame is shown in Fig. 28.

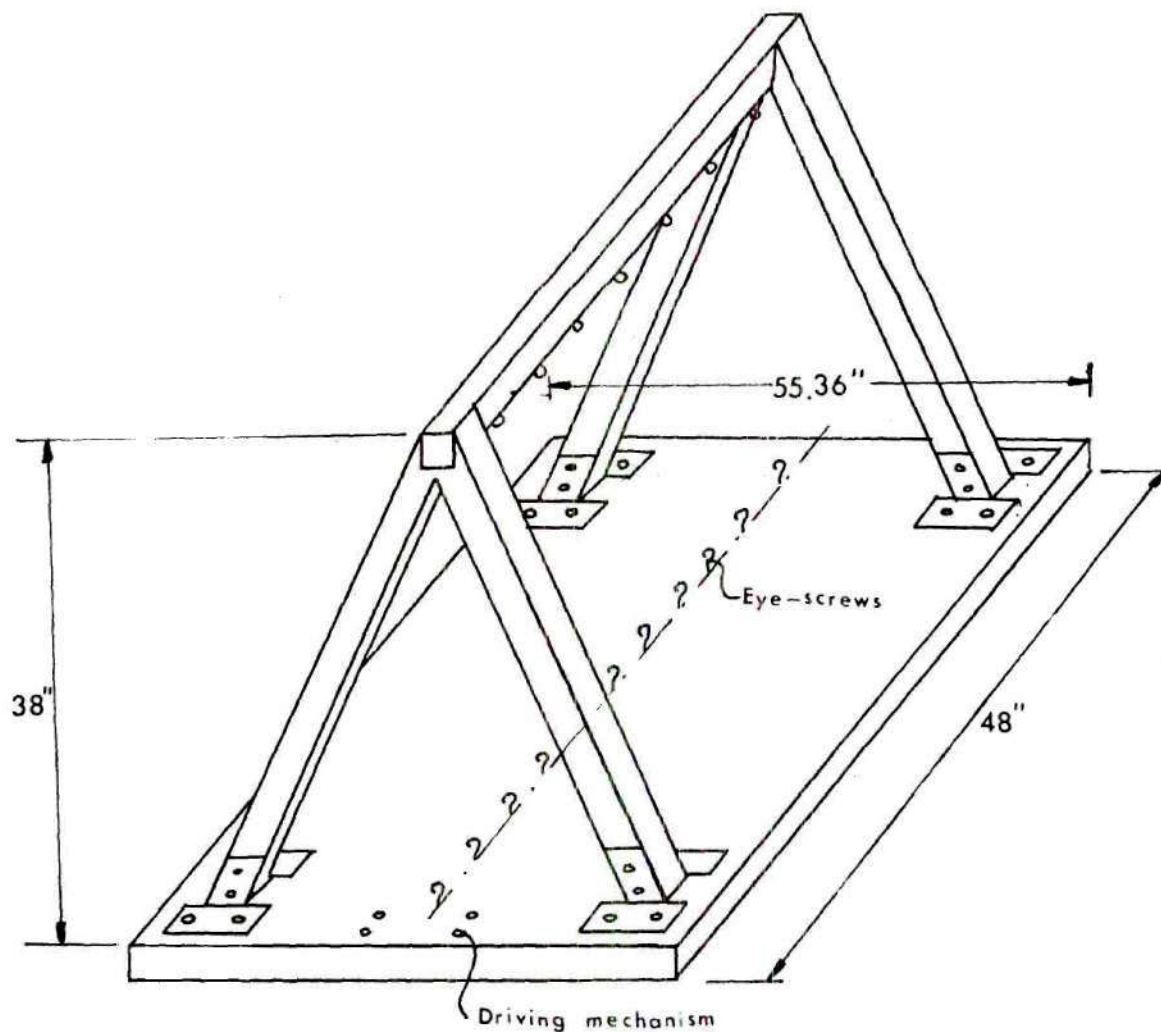


Figure 28. Frame of the Model

Photographs of the model are included in Figures 29a, 29b, 30 and

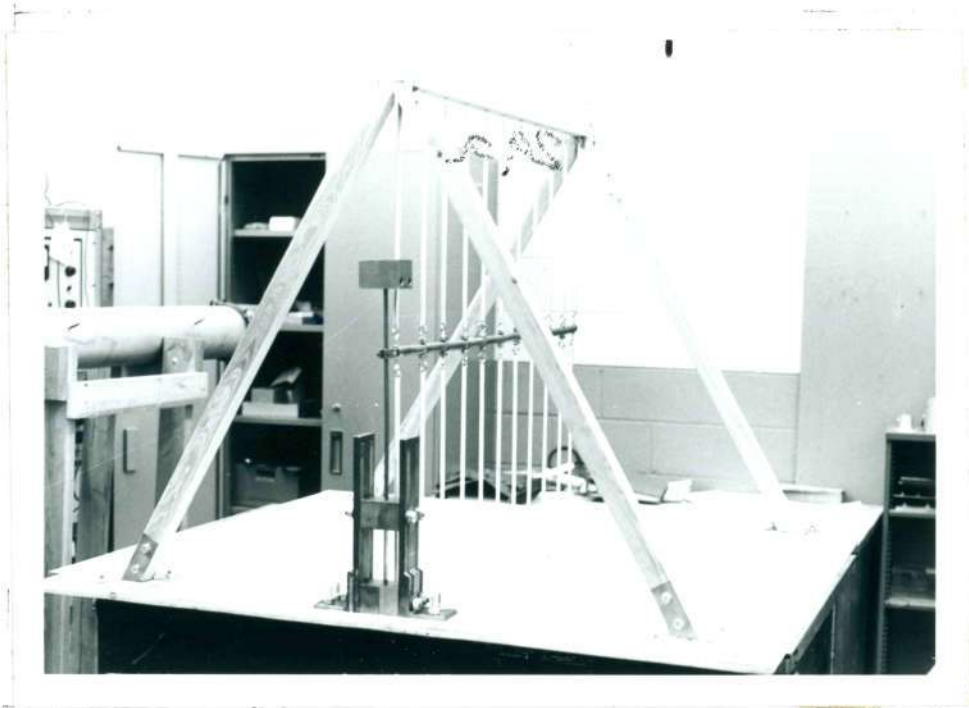


Figure 29a. Experimental Model

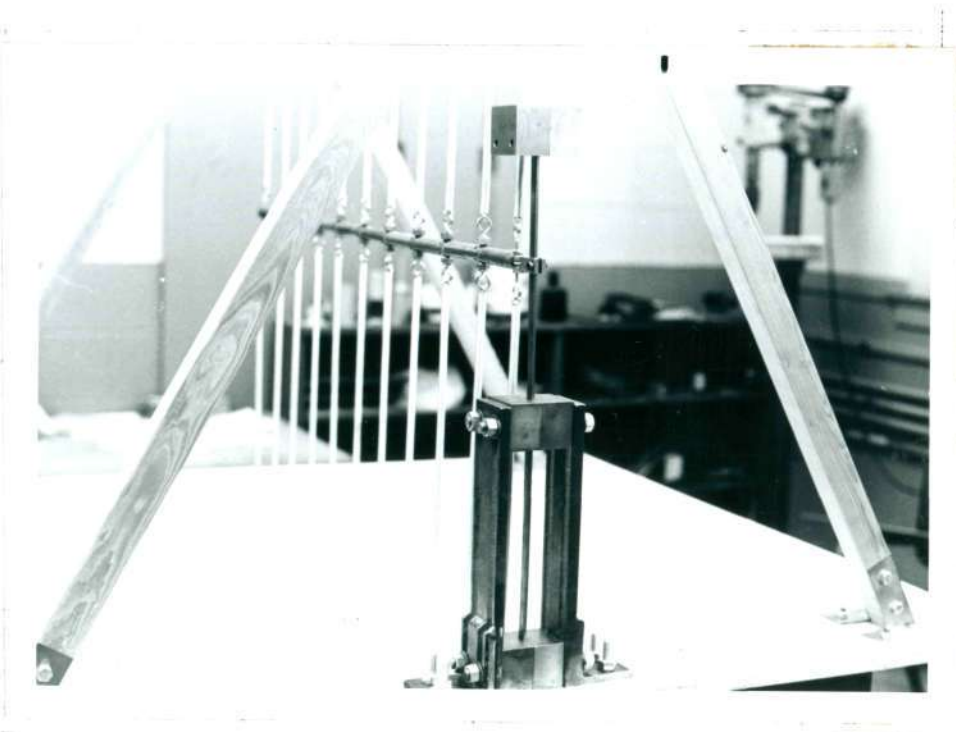


Figure 29b. Experimental Model

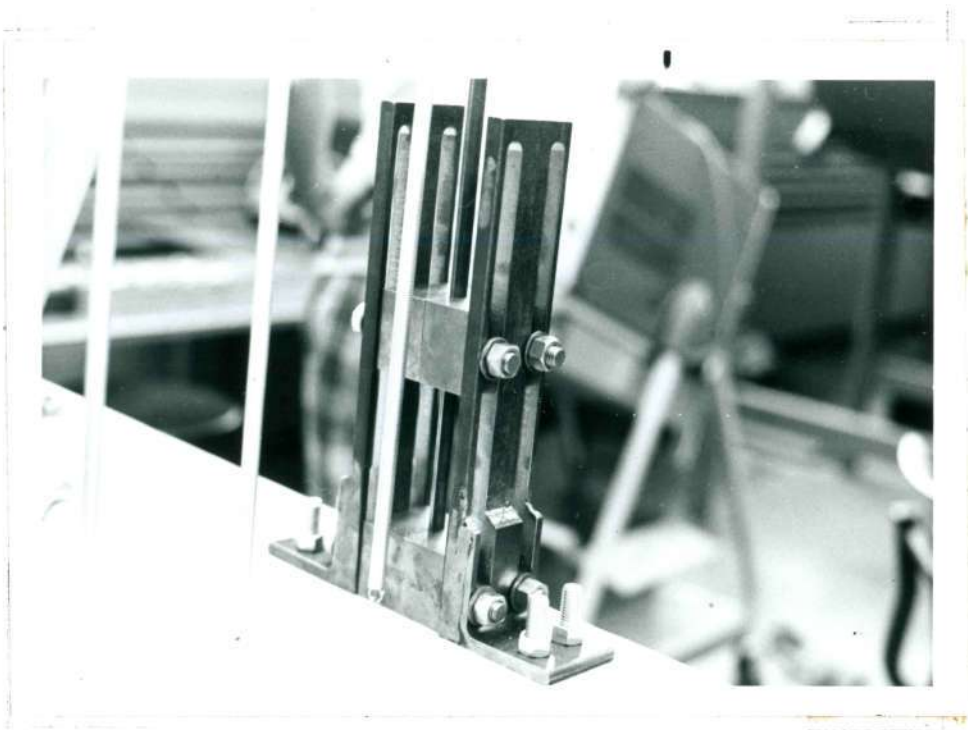


Figure 30. Driving Mechanism



Figure 31. Coupling of Beam to Chain

## CHAPTER IV

## DATA AND COMPARISON WITH THEORY

After the experimental model was built, several observations were made. The goal was the collection of data of the same kind as that resulting from the calculations in order that one could compare the theoretical results with the experimental data. In other words, the idea was to measure the amplitude displacements of all the joints on the chain, for various values of the parameter  $\delta$ .

Before any measurement were made, it was necessary to check the experimental response of the driving mechanism. This was found to be slightly different from that of the theoretical calculations. In order to compare the theoretical and experimental response of the mechanism, graphs were plotted of the driving frequency  $f_{nb}$  as a function of the length of the cantiliver beam.

The theoretical predictions follow from Eq. (63)

$$\omega_{nb}^2 = \frac{3EI}{l^3 \left(m + \frac{mb}{4}\right)} \quad (63')$$

where

$$\omega_{nb}^2 = 4\pi^2 f_{nb}^2$$

thus

$$f_{nb}^2 = \frac{3EI}{4\pi^2 l^3 \left(m + \frac{mb}{4}\right)}$$

which with the appropriate numerical substitution becomes

$$f_{nb}^2 = \frac{3 \cdot 30 \cdot 10^6}{12 \cdot 2^{10} \cdot 4\pi \cdot 1^3 \left( \frac{4}{g} + \frac{0.0175}{4g} 1 \right)} = \frac{185 \cdot 386 \cdot 4}{1^3 (16 + 0.0175 \cdot 1)}$$

or

$$f_{nb} = \sqrt{\frac{14.26 \cdot 10^4}{1^3 (16.0 + 0.0175 \cdot 1)}} = \frac{532}{1} \cdot \frac{1.0}{16 \cdot 1 + 0.0175 \cdot 1^2}$$

Table 7 gives the theoretical and experimentally observed frequencies of the beam for different values of  $l$ .

Table 7. Beam Frequencies

Beam Length $l$ (in)	Theor. Frequency $f_{bt}$ ( Hz )	Exp. Frequency $f_{be}$ ( Hz )
20.62	1.40	1.34
19.75	1.47	1.39
18.06	1.72	1.43
17.18	1.87	1.50
15.62	2.13	1.75
14.25	2.44	2.00
13.00	2.82	2.25
12.25	3.09	2.42
11.81	3.26	2.67
11.00	3.64	3.00
10.50	3.90	3.17
10.00	4.21	3.50

Figure 32 gives the theoretical and experimental curves of the beam frequency as a function of the beam length.

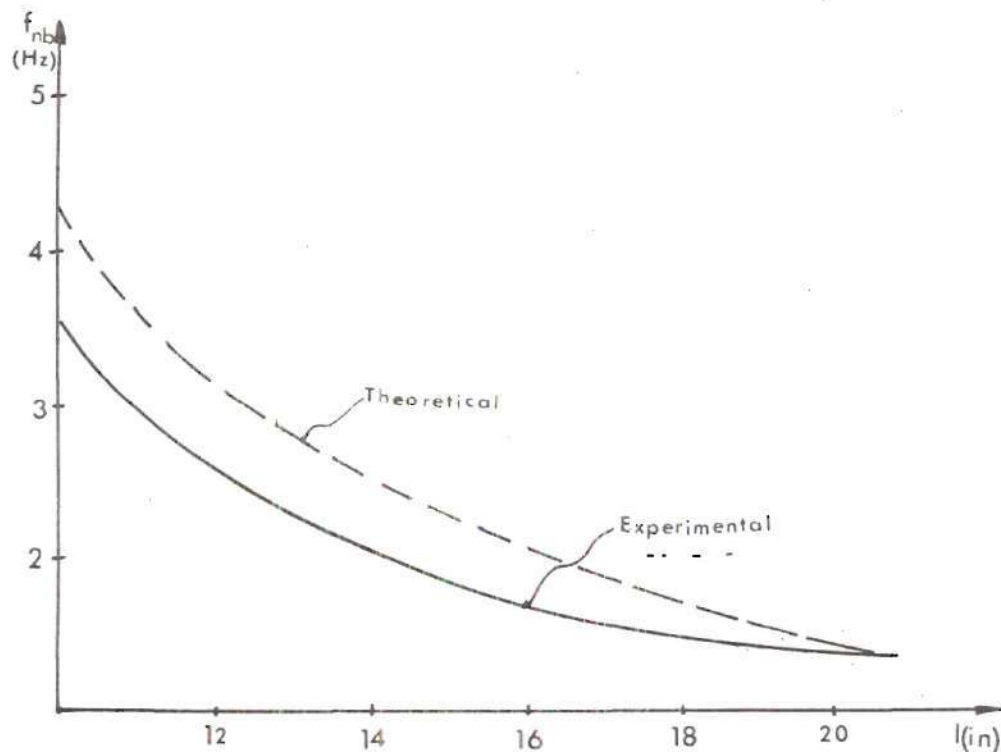


Figure 32. Beam Frequency Vs. Beam Length

The experimental curve in Fig. 32 suffices for the calibration of the mechanism. For any desired frequency, it predicts the corresponding length of the cantiliver beam. This length is a parameter that can be measured and fixed without difficulty in the experimental model.



### Experimental Results

The results obtained from different experiments with the model are not of a quantitative value since no numerical data was collected. However, many observations were made and the resulting photographs show the pertinent qualitative results of the experiment.

It was not possible to collect any numerical data regarding motion of the chain for different input frequencies. The principal reason for this is the relatively small amplitude of displacement of the joints on the chain. If one refer back to Table 4, which shows the theoretical results for a case similar to the experimental case, i. e.  $\Psi = 0.5$ , it is found that the range of the amplitude ratios:  $X_i + 1/X_1$  goes from a value of 2.02 to  $3.5 \times 10^{-11}$ . Considering that the values for  $\bar{X}_1$  in the model are not larger than 1.5 in., the measurement of such small amplitude displacements along the chain was beyond the present capability of the available equipment.

The observations along with the corresponding photographs show the response motion of the chain in the experimental model for excitation with different driving frequencies. These have values ranging from 1.5 to 4.2 Hz/sec.

These results are for the most part compatible with the theoretical prediction. It is possible to see that at frequencies below the characteristic frequency of the system (approximately 2.7 Hz/sec), i. e. 1.5, 1.85, 2.40 Hz/sec, all the joints on the chain have displacements of the same sign that the initial displacement at any time. The amplitude of the displacements decrease at successive joint down the chain. This is compatible with the analytical results given in Table 4 for values of  $\delta$  equal to 1.5, 2.0, 3.0, 5.0.



The journal friction on the joints considerably affects the response motion. This effect is especially noticeable at low values of the disturbance frequency. When this frequency adopts values above 4 Hz the effect is not as significant. For this last case, the observations were made after a manual perturbation was given to the chain since the driving mechanism works only up to 3.5 Hz.

All the photographs were taken using a Minolta SRT 101 Camera with a f 1.7 lens. The film used was black and white prints, Kodak 135-20 with ASA 400. The camera was set up on a tripod 4 feet above the lower frame level. The axis passing through the lens made a  $20^\circ$  angle with a vertical axis, perpendicular to the chain. The exposure time was set at  $1/125$  sec.

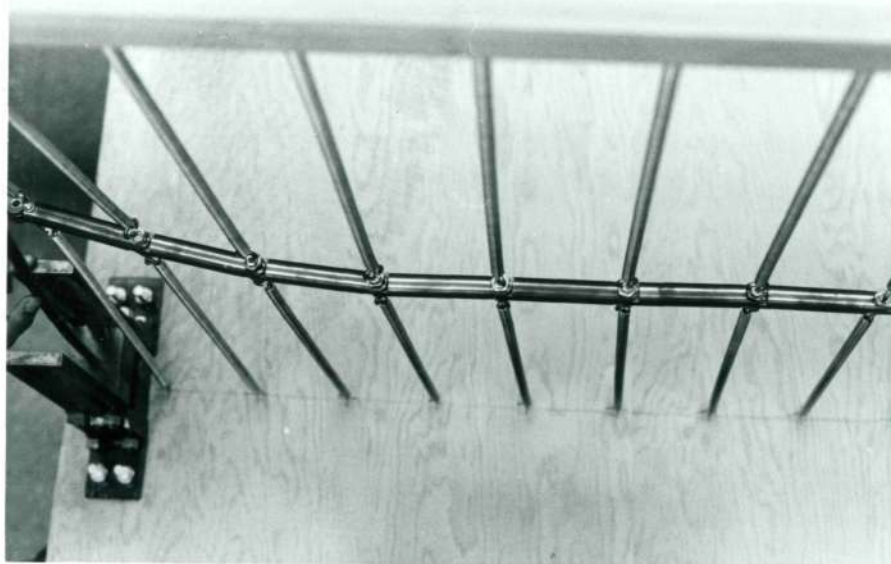


Figure 33. Response Motion for  $f = 1.5$  Hz

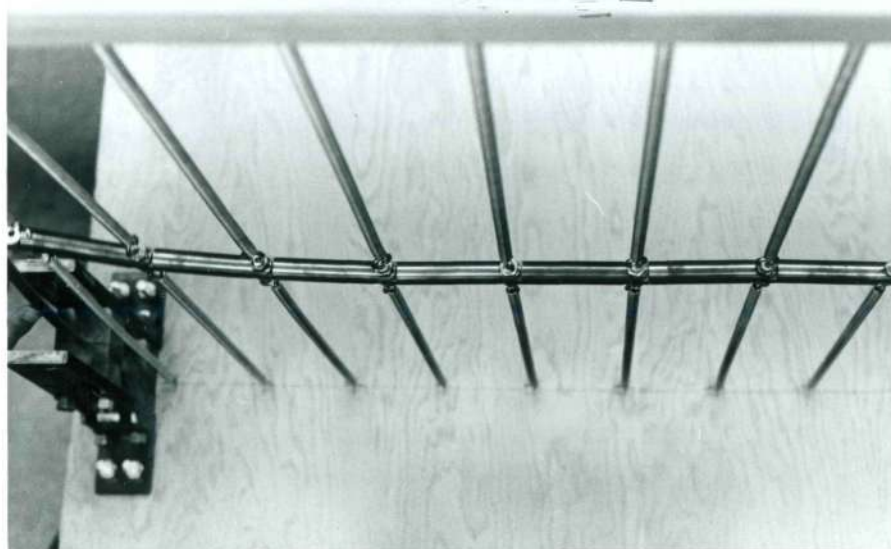


Figure 34. Response Motion for  $f = 1.85$  Hz

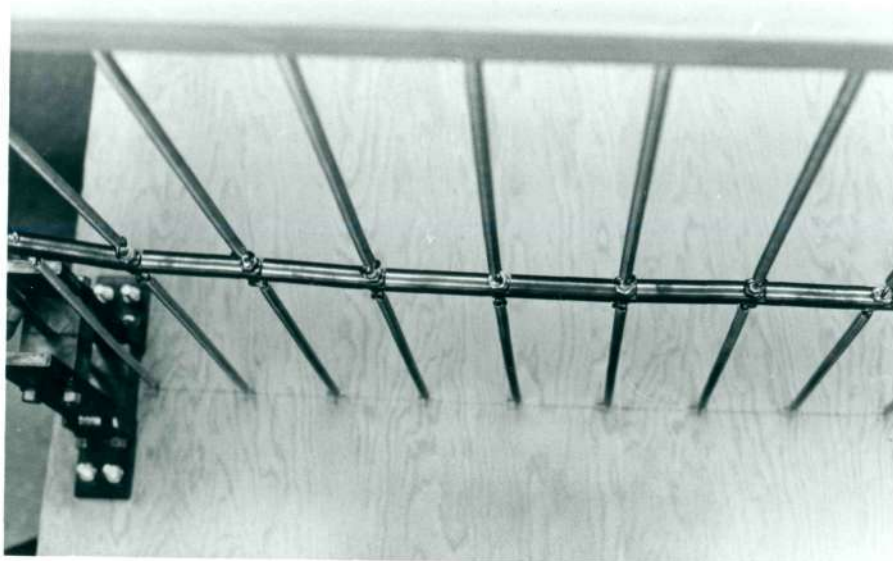


Figure 35. Response Motion for  $f = 2.4$  Hz



Figure 36. Response Motion for  $f = 2.75$  Hz



Figure 37. Response Motion for  $f = 3.1$  Hz

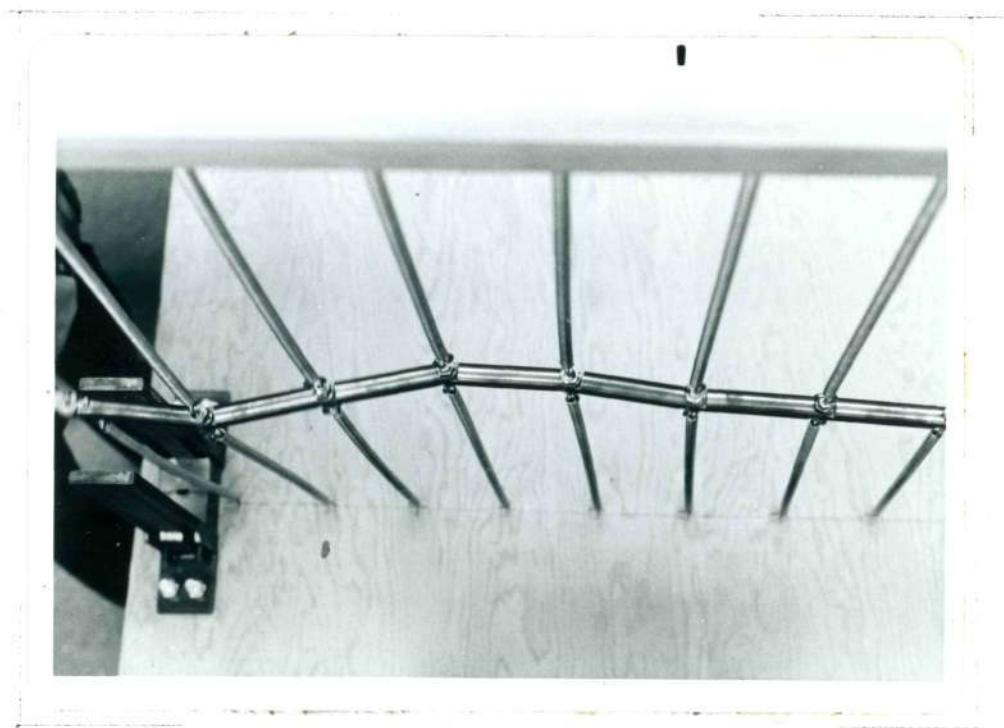


Figure 38. Response Motion for  $f = 3.5$  Hz



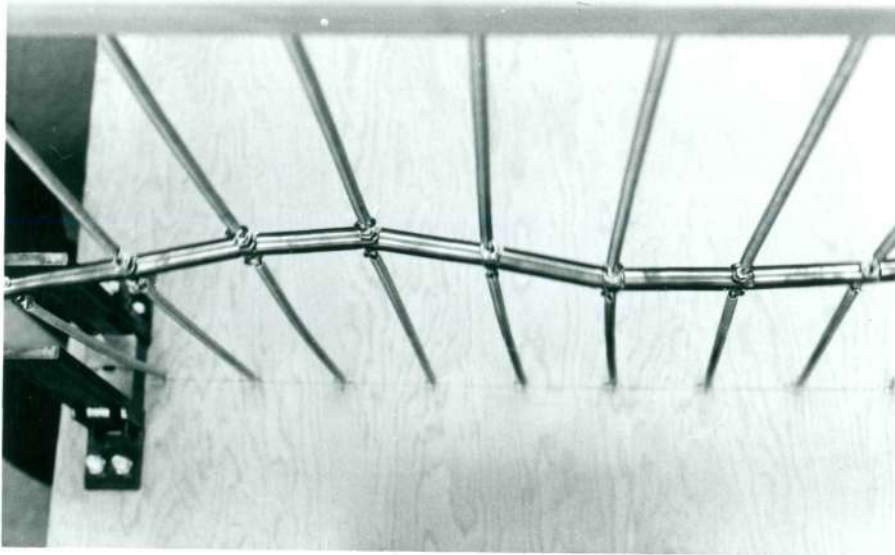


Figure 39. Response Motion for  $f = 4.0$  Hz

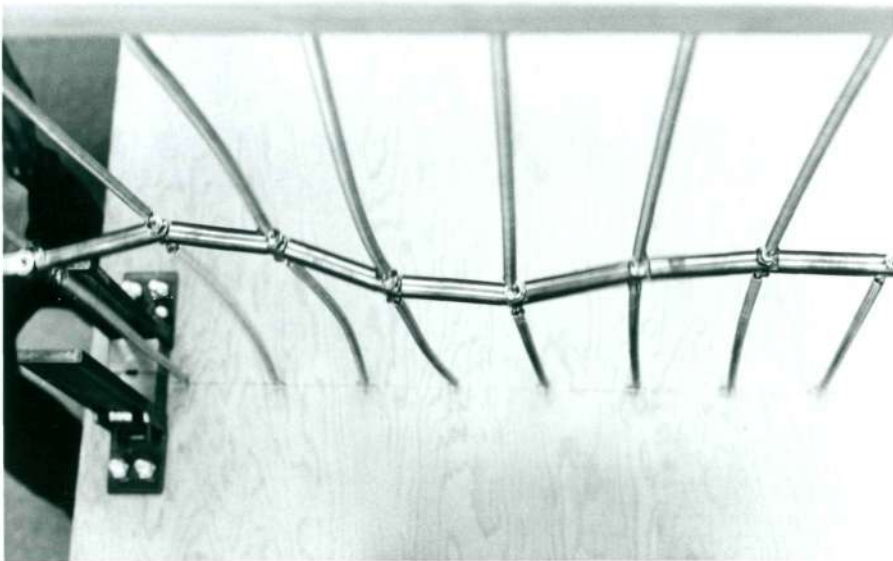


Figure 40. Response Motion for  $f = 4.5$  Hz

## CHAPTER V

## DISCUSSION AND CONCLUSIONS

The present research has two well defined parts: (1) the analytical derivation, and (2) the observations on the experimental model. An effort was made to present both parts in as close a relation as possible. However, some comments may be made concerning the relation of the two.

The mathematical model was chosen with several assumptions and simplifications. The reason for this was that we have a sufficiently simple model that we could have relatively uncomplicated solutions. These solutions were obtained, although they are not completely in agreement with the actual model. The reason for the incomplete agreement are as follows:

1. The individual elements of the chain are not perfectly right and may deform a small amount. One implication this neglect may be found in the graphs in Figs. 13, 14, 15, and 16, which give the motion response of the chain. When the amplitude is sufficiently large one would expect each element to be stretched a different amount, especially when the values of  $\delta$  are above 1.0. This is a clear disagreement with the experiment model, where all the elements of the chain may not stretch sufficiently to insure that the motion of each joint be perfectly transverse. In the actual model, the chain when undergoing the motion shown in the photographs is

alternately undergoing a net longitudinal shortening of length. This was not considered in the mathematical model.

2. When considering the mathematical model, we assumed no friction forces on the joints. The experimental model has a metal to metal friction on the joints, and the correspondent friction forces. This is a very important parameter, very influential in the motion transmission along the chain.
3. In the experimental model, due to the size of the rods, the nature of the designed joints and of the eye-screws holding the elastic members, the length of individual members is significantly different than assumed by the theory. Also the inertial effects of these parts of the system were not considered in the derivation.

The most important results of this study was the determination of that value of the parameter  $\delta$  which represents the border between two significantly different response motions of the chain. This value was found to be unity which is when the driving frequency is equal to the characteristic frequency of the system. For any future research on this topic, it is recommended that one introduce some changes in the mathematical model.

For instance, one should consider the longitudinal shortening of the chain when transverse motion is present. Also, friction forces must be included in the force analysis in the derivation. Finally, a reduction in the number of elements of the chain up to five or six rods might be tried.

Practical applications for this system were not considered in



this study. However, the system represents a prototype of a mechanical filter with strong frequency dependent characteristics. Such a filter might be useful in any application where only frequencies above some given value are desired to be transmitted.

## APPENDIX I

The program used for successive matrix multiplication is listed below in Fortran IV Language

```

FOR , IS MATMULT. MAIN
C   PATRICIO ALBAN
      DIMENSION A (3,3), B (3,3), C (3,3)
      DATA C/9 * 0.0 /
      READ 10, N
10   FORMAT ( )
      M = 0
      READ 20, ( ( A ( I, J), J = 1, 2), I = 1,2)
20   FORMAT ( )
      DO 100 I = 1,2
      DO 100 J = 1,2
100  B (I, J) = A (I, J)
140  M = M + 1
      DO 110 I = 1,2
      DO 110 J = 1,2
      DO 110 K = 1,2
110  C (I, J) = C (I, J) + A (I, K) * B (K, J)
      IF (M .GE. N) GO TO 120
      DO 130 I = 1,2
      DO 130 J = 1,2
      A (I, J) = C (I, J)

```

```
130 C (I, J) = 0
```

```
GØ TØ 140
```

```
120 PRINT 30, ( ( C (I, J), J = 1,2), I = 1,2)
```

```
30 FORMAT ( / / , 5 x , 2 F1 5.2)
```

```
END
```

## BIBLIOGRAPHY

1. Nakada, T. "Mechanical High-Pass Vibration Filter Applying Bifilar Pendulum," unpublished paper, Tokyo Institute of Technology, 1970.
2. Kane, T. R., and Gan-Tai-Tseng. "Dynamics of the Bifilar Pendulum," International Journal of Mechanics and Science. Pergamon Press Ltd. 9:83-96. Great Britain, 1967.
3. Den Hartog, J. P. Mechanical Vibrations, McGraw-Hill Book Company, New York, 1956.

## OTHER REFERENCES

Greenwood Donald T., Principles of Dynamics. Prentice-Hall Inc., Englewood Cliffs, New Jersey, 1965

Seto William, W., Mechanical Vibrations, McGraw-Hill Book Company, Schaum's Outline Series, New York, 1964.

Sloane Alvin, Mechanics of Materials, Dover Publication Ind., New York, 1952.